AUTONOMIC SIGNAL PROCESSING DURING G.I. STIMULATION

PROCESSING OF

AUTONOMIC SIGNALS DURING GASTROINTESTINAL STIMULATION

IN HUMAN SUBJECTS

By

HARJEET SINGH BAJAJ, B.Eng & Mgt

A Thesis

Submitted to the School of Graduate Studies

in Partial Fulfillment of the Requirements

for the Degree

Master of Applied Sciences

McMaster University

MASTER OF APPLIED SCIENCES (2005) **McMaster University**

(Electrical and Computer Engineering) Hamilton, Ontario

TITLE: Processing of Autonomic Signals during Gastrointestinal Stimulation in Human Subjects.

AUTHOR: Harjeet Singh Bajaj, B.Eng. & Mgt (McMaster University)

SUPERVISOR: Markad V.Kamath, Ph.D., P.Eng.

NUMBER OF PAGES: xii, 103

ABSTRACT

Gastro-intestinal stimulation using a rectal balloon distended with an inflation device is often used to investigate patients with Irritable Bowel Syndrome (IBS). The acquisition and processing of hemodynamic signals from healthy controls and IBS patients during colo-rectal distension is explored in this thesis. Rectal stimulation was performed using a barostat system run on a labview platform. The rectal pressure (using balloon) increased gradually to a user controlled maximum value, held at a 50% discomfort level, followed by a phasic drop in pressure. A baseline and recovery period was used before inflation after deflation states respectively. The blood pressure and heart rate signals were recorded and beat-to-beat variations of these signals were computed. The autonomic signals embedded in the beat-to-beat variations of the hemodynamic variables subjected to power spectral analysis, Wigner-Ville analysis and to the computation of the baroreceptor sensitivity. The objective of the study was to develop signal processing methods to evaluate the autonomic nervous system. Results show that rectal balloon distention perturbs the human ANS and is a powerful tool into assessing the nature of the ANS response in human subjects. Novel methods of studying heart rate and blood pressure using empirical mode decomposition are also proposed.

Acknowledgements

In particular, I would specially like to thank my supervisor Dr. M.V. Kamath as his mentorship and guidance was of great assistance through out my graduate studies. A special thanks also to Dr. Robert Spaziani for his willingness to offer clinical and physiological advice as well as support through humor during the grueling studies. A sincere thanks to Keith Redmond for his insightful discussions.

I would like to especially thank my parents, sisters and brother for their support and help over the past two years. A special thank you to my father for being a great role model to live up to and an inspiration. A special thank you to Regi, Tanya, and Jennifer, and Sonia for their helpful feedback.

I wish to express my thanks to DeGroote Foundation and Natural Sciences and Engineering Research Council for their support of this work. The equipment support by Astra Zeneca, Sweden (Dr.Alfred Bayati) is gratefully acknowledged. I also thank all healthy control subjects and patients who participated in the study. A special note of thanks to Dr. Gervais Tougas who provided initial support and to Dr. S.Collins who gave the continuing assistance during this work.

Contents

LIST OF ILLUSTRATIONS AND DIAGRAMS

LIST OF TABLES

LIST OF ABBREVIATIONS

ANS Autonomic Nervous System

BT Blackman-Tukey

BPV Blood Pressure Variability

BRS Baroreceptor Sensitivity

DBP Diastolic Blood Pressure

EMD Empirical Mode Decomposition

GI Gastrointestinal (system)

HRV: Heart Rate Variability

IBS Irritable Bowel Syndrome

IBD Inflammatory Bowel Disease

PSD Power Spectral Density

SBP Systolic Blood Pressure

WV Wigner-Ville method for computing time frequency

Chapter 1

BACKGROUND ON IRRITABLE BOWEL SYNDROME

1.1 INTRODUCTION

Irritable bowel syndrome (IBS) is one of the most common functional gastrointestinal (GI) disorders worldwide that is characterized by abdominal pain and altered bowel habits in the absence of any demonstrable organic pathology [18]. The cause of this debilitating syndrome which affects approximately six million Canadians is not well understood. There are few, if any, studies documenting effective therapies to treat IBS. The symptoms of IBS, which are usually chronic, include abdominal pain or discomfort, bloating, cramps, and altered bowel movement resulting in constipation, diarrhea or alternation between these two extremes. IBS is a collective term used to

represent this GI disease. Although each patient has a unique experience with symptoms of IBS, a significant reduction in quality of life is common for all sufferers of IBS.

Although the causes of IBS are not well known at present, the effects of IBS on the muscle of the large bowel or colon have been studied. Individuals with IBS have an altered intestinal muscle contraction (motility) pattern. In spite of the chronic pain, IBS does not cause an increased risk of more serious bowel diseases such as inflammatory bowel diseases or colon cancer. There are many theories for the causes and factors that trigger IBS episodes. Dietary issues including food allergies and the amount of fibre intake, physical exercise, and stress level are commonly considered contributing factors to IBS. Use of antibiotics, chronic alcohol abuse, and bile acid mal-absorption are some of the other possible causes Abnormalities such as gastrointestinal infections or abnormalities in the GI secretion and/or peristalsis are some other possible causes of IBS. A unique hypothesis which is currently being explored by several investigators to the possible cause and trigger of IBS stems around the concepts of neurological hyper-sensitivity and autonomic nervous system impairment.

1.2 DEMOGRAPHICS

The prevalence of IBS in some populations is reported as high as 30%. It is estimated to affect 13- 20% of all Canadians. IBS affects individuals of all ages and from all walks of life. Episodes may occur during childhood or adolescence, and may resolve during a certain period of a lifespan and then reoccur at any age. Demographic studies suggest that 70% of the sufferers are women. Women are twice as likely to have IBS at some point in their life as compared to men [18]. Greater than 85% of IBS sufferers

experience symptoms that have a negative impact on work, traveling and socializing. When asked to explain the effect on the quality of their lifestyle, 45 percent of those polled stated that IBS has had a severe impact on their quality of life. In addition to deteriorating quality of life, IBS also has a negative economic impact. IBS is the second leading cause of absenteeism from work or school behind the common cold.

1.3 DIAGNOSIS

The symptom criteria for IBS include the feeling of abdominal pain or discomfort, which is either relieved during defecation or alters the frequency and/or consistency of the stool. In addition, an irregular pattern of defecation is prevalent at least 25% of the time with at least three of the following conditions: altered stool frequency, altered stool form (hard or loose stool), altered stool passage (staining or urgency, feeling of incomplete evacuation), passage of mucus, and/or bloating or feeling of abdominal distension [18]. These symptoms are usually prevalent continuously or recurrently for a period lasting three months or more. Since these symptoms are quite varied, there are very few objective tests to determine if a patient has IBS. As a result, part of the diagnosis process is to rule out other known diseases.

1.4 SIGNAL PROCESSING AND THE INVOLVEMENT OF THE AUTONOMIC NERVOUS SYSTEM IN IRRITABLE BOWEL SYNDROME

The autonomic nervous system (ANS) is an extensive network of neurons whose main function is to regulate the *milieu interieur* by controlling homeostasis and visceral functions. Although most functions that are regulated by the ANS are controlled unconsciously, emotions and somatosensory inputs do have a profound influence on the

ANS. In addition, the ANS plays a significant role in pain modulation and perception. The peripheral components of the ANS are the sympathetic and parasympathetic nervous systems. These two systems usually oppose each other, especially as measured on the hemodynamic control.

In 1928, it was first proposed that IBS could be related to an imbalance in the ANS. This idea remained unexplored until the 1990's, when ANS was included in the models of IBS based on the hypothesis that alterations in the extrinsic innervations might account for disturbance in motility and/or visceral sensitivity. Both of these are considered to be contributing factors to the etiology of IBS. Studies have been performed on IBS patients to determine contributions due to autonomic dysfunction, using non-invasive techniques that quantify the ANS balance [29].

Current models of IBS pathophysiology link the central nervous system to the enteric nervous system through the ANS. As a result, it was possible to realize that changes in the ANS could modulate motility, resting muscle tone and pain transmission. Based on past studies it has been observed that constipated IBS patients reveal a low vagal tone and diarrhea IBS patients exhibit an augmented vagal tone [29].

Non-invasive techniques to assess the ANS involve the assessment of heart rate variability (HRV) measures. Power spectral analysis of the HRV can be used as a tool for determining the sympathetic and parasympathetic nervous system balance. The techniques used to compute the power spectral analysis vary depending on the underlying characteristic of the data stream and the assumptions inherent from the paradigm construct. For linear, stationary data streams, the Blackman Tukey (non-parametric) and Autoregressive (parametric) methods of power spectral analysis were used. For data

deemed non-stationary Wignerville Distribution was examined. This time-frequency analysis method allowed for a three dimensional perspective of the power magnitude across both frequency and time. In order to determine the shifting of frequency components and to observe the predominant frequency component, the Empirical Mode Decomposition method (a method which does not assume linearity or stationarity of data) is proposed in this thesis.

In addition to assessing the peripheral components of the ANS, the ANS itself was indirectly assessed via the baroreceptor reflex (BRR). The BRR is a control system which modulates the heart rate in response to the change in blood pressure in order to regulate the blood flow. Three different methods were used to compute the baroreceptor sensitivity (BRS) values. The three-point method was used as the time domain method. Robbe's and Pagani's methods were the frequency domain BRS methods used [3,7,10,16].

1.5 GASTRO INTESTINAL STIMULATION

Rectal balloon stimulation was used to emulate the filling of the bowel. The balloon was controlled by a barostat controlled by a PC. Physiological variables collected included heart signal, blood pressure, respiration, balloon pressure and balloon volume. The distension paradigm used for these studies involved four states: baseline, ramp, tonic and post. Detailed description of the system and the paradigm used are provided in subsequent chapters.

1.6 OVERVIEW

Results of our study show that the ANS is implicated in IBS. During the balloon distention, the autonomic nervous system revealed augmented measures of ANS. The BRS provided further insight into the ANS impairment of the patients group. The BRS values were significantly lower for patients when compared to the controls.

Chapter 2

AUTONOMIC TESTING OF PATIENTS WITH IBS: A LITERATURE REVIEW

2.1 INTRODUCTION

Studies reported in this thesis were performed to investigate the autonomic effects of distentions in patients with functional IBS and in healthy controls (HC). The primary objective of this thesis is to provide a perspective to this requirement by studying and exploring the autonomic responses (BP, ECG) of both IBS patients and healthy controls. A symptom based criterion developed by multinational working teams (Rome Committees: [18] was used for identifying the IBS subjects. However, specific and reliable biomarkers that show an accurate correlation with subjective symptoms are generally not available.

2.2 DESCRIPTION OF PROBLEM

The ANS response (BP change and ECG evaluation) has not been studied in the past for IBS although there are some recent publications in the field [29]. These studies suggest that IBS subjects do differ from healthy controls with respect to the autonomic balance [29]. The primary objective of this thesis is to use non-invasive digital signal processing techniques to explore the autonomic responses (BP, ECG) of IBS patients and healthy controls undergoing colorectal distensions. Since it has been suggested that lowered sensory thresholds may be surrogate markers for chronic visceral hyperalgesia in patients of IBS, the sensation responses were recorded during the study using an electronic analog scale. This information was used during the analysis stage to dissociate the IBS patients from the healthy controls.

2.3 IMPORTANCE OF ANS IN IBS

The autonomic nervous system is part of the nervous system that regulates the basic visceral processes that are needed for the maintenance of normal bodily functions. It operates independent of voluntary control. However certain events, such as emotional stress, fear, sexual excitement, and alterations in the sleep-wakefulness cycle, can change the level of autonomic activity.

The autonomic system consists of three major components: the sympathetic nervous system, the parasympathetic nervous system and the enteric nervous system. The sympathetic and parasympathetic nervous systems often function in antagonistic ways. The enteric nervous system consists of a collection of neurons embedded within the wall of the entire gastrointestinal tract. This system controls gastrointestinal motility and

secretions. The ANS also regulates the movement and functions of the stomach, intestine and salivary glands, the secretion of insulin and the urinary and sexual functions. The ANS acts through a balance of its two components, the sympathetic nervous system and parasympathetic nervous system.

In our study, we have evaluated the sympathetic and parasympathetic nervous system for possible source of dysfunction. In addition, the ANS is responsible for inducing emotional responses to a given situation (fear, anxiety, sadness, joy etc) which are strongly influenced by the sensory perception of peripheral changes in the viscera.

2.4 DESCRIPTION OF ANS TESTING IN THE LITERATURE

Several methods of testing the Autonomic Function have evolved over the years. Standardized testing methodologies have been developed which allow for the testing of the sympathetic and parasympathetic nervous system. The testing modalities available most widely are those that record heart rate and blood pressure. The heart rate is determined based on the recording of the electrocardiogram. Non-invasive methods have been developed to circumvent the difficulty and discomfort associated with the invasive approach of inserting an arterial line. Plethysmographic recording of arterial blood pressure pulse waves from a digit or from the radial pulse at the wrist can be performed with minimal discomfort for the patient. This advance allows for instantaneous recording of blood pressure and pulse rate, and therefore, standardized tests of baroreflex function are now possible on a routine basis.

Non invasive methodologies that use blood pressure and heart rate measure for determining the ANS function include the tilt table test, the Val Salva Maneuver,

Quantitative Sudomotor Axon Reflex Test (QSART) among others. The tilt table test requires that the patient lie on a table that is then raised. The Val Salva maneuver requires that the patient blow into a tube to increase pressure in the chest, and the QSART involves measuring the sweating and skin temperature. While these simple tests are performed, blood pressure and heart rate are monitored. Determining the ANS function includes the tilt table test, the Val Salva maneuver and the QSART.

2.4.1 Tilt Table Testing [7]

The indication for such testing is usually episodic alteration of consciousness, most often associated with assumption of an upright position from a horizontal or seated position. As noted above, tilt-table testing is part of the evaluation of syncope. It is performed by having the test subject lie on a motor-driven tilt table. The heart rate and blood pressure are monitored for 5 to 15 minutes while the patient lies quietly. Once stable recordings are made, the head of the table is tilted up to 60^{o}, and the heart rate and blood pressure are monitored for up to 40-45 minutes. A normal response is a brief, transient decrease in blood pressure accompanied by an increase in heart rate. There is a return to near-baseline rates and pressures, and this is maintained throughout the period of tilting.

Several abnormal patterns can be recognized. Patients who experience neurocardiogenic syncope will have normal initial responses, but develop bradycardia and progressive hypotension after 15-20 minutes of tilting. Patients with multiple system atrophy or pure autonomic failure exhibit no change in heart rate in response to tilting, but their blood pressure progressively declines throughout the period of tilting.

2.4.2 Val Salva Maneouver

In addition to tilt-table testing, the baroreflex arc can be assessed by having the patient perform paced deep breathing and Val Salva maneuver while blood pressure and heart rate are recorded. When a normal individual takes regular, deep breaths at a rate of 5-6 breaths per minute, the heart rate and blood pressure are entrained in a sinusoidal fashion. The degree of heart rate variation is a mainly a measure of parasympathetic tone on the cardiac conduction system. The degree of heart rate variation is averaged over 5 breathing cycles and is compared with age-adjusted normal values.

The Val Salva maneuver is performed by instructing the patient to forcibly exhale into a manometer. The objective of this test is to increase intrathoracic pressure. The test is standardized by instructing the patient to achieve a pressure level of 40 mm Hg. A small air leak is created in the manometer system in order to avoid an artifactual increase in the exhaled pressure. This is done to insure that the exhaled pressure is due to the contraction of the expiratory muscles and not from the pressure generated by the buccal muscles. The exhaled pressure is maintained for 15 seconds and then is rapidly released. The normal response would demonstrate a dynamic interaction between the pulse rate and the blood pressure. For example a normal response would reveal a decrease in blood pressure during the forced exhalation, accompanied by a reflex increase in heart rate. After release of the pressure, there would be a rebound in the blood pressure followed by a reflex slowing of the heart rate. The Val Salva ratio is calculated as the ratio of the fastest heart rate to the slowest heart rate after its release during the Val Salva maneuver.

This value can also be compared with age-adjusted norms. The heart rate and blood pressure changes that occur during the Valsalva maneuver are largely due to the sympathetic nervous system.

2.4.3 QSART

The Quantitative Sudomotor Axon Reflex Test (QSART) is yet another autonomic test which is performed by measuring the sweating and skin temperature. The QSART is used to assess the small nerve fibers that are linked to the sweat glands. The objective of QSART is to diagnose the disturbances of the ANS, which controls the sweat glands, heart, blood pressure, and also the digestive system along with other organs. The test measures the resting skin temperature, resting sweat output, and the stimulated sweat output. These measurements are taken usually on the arms or legs. The temperature and the amount of sweat under the skin are measured by positioning a plastic container on the skin. A chemical is delivered electrically through the skin to a sweat gland, in order to stimulate sweat. The data obtained is digitally recorded and analyzed in order to determine how functionality of the nerves and sweat glands.

2.5 ROLE OF HRV, BPV

Cardiovascular fluctuations can be studied via beat- to- beat heart rate and blood pressure monitoring and calculation of the variance of their average values. In order to extract additional information from the beat to beat signals, frequency domain analysis has been introduced to subdivide the variability of the blood pressure and heart rate into frequency components and to quantify the power (variance) across the frequency spectrum. A wide variety of algorithms have been developed to study instantaneous

cardiovascular variability and models that characterize the relationships between changes in heart rate and blood pressure [9].

Eighty year ago, Hales and von Haller initially described the rhythmic BP and HR oscillations as corresponding to respiratory activity [2]. Mayer later proposed that BP had slower oscillations (than the respiratory rhythm) which were related to vasomotor activity. More recently, sophisticated techniques have been developed that utilizes digital data acquisition and signal processing methods to perform power spectrum analysis. Observation of power spectrum analysis of HR and BP signal have led to the discovery of three predominant peaks; low frequency (LF) 0.04-0.15 Hz, high frequency (HF) 0.15 – 0.50 Hz, and very low frequency (VLF) 0-0.04 Hz. The low frequency region is mainly correlated to the sympathetic system and the high frequency corresponds to the parasympathetic system [2,14,20,21,26,27].

There are some investigators that believe that the focus of the analysis of the graphs should be on peak detection since they feel that a peak may reflect a specific cardiovascular control mechanism that can be assessed as the power under just that peak. However, observations suggest that a peak may originate from more than one cardiovascular control mechanism and that a single cardiovascular mechanism may contribute to more than one peak. Also, recent studies have revealed that BP and HR include not just rhythmic, but also non-rhythmic oscillations. These non-rhythmic oscillations do not appear as clearly defined peaks, but as powers spread over a frequency band. It is clear that non-rhythmic oscillations also have relevance to cardiovascular control mechanisms. This has been demonstrated by a study performed on unanesthetized cats. The removal of the baroreceptor restraint of the sympathetic activity by sinoaortic

denervations reveals systematic changes in nonpeaked BP and HR powers in several frequency regions. In humans, normotensive and hypertensive subjects alike showed systematic modification of the non-peaked BP and HR powers during sleep state; a state when the sympathetic activity is reduced and the vagal activity increased

2.5.1 Interpretation of Indices Derived from Heart Rate and Blood Pressure Variability

Vagal cardiac control operates like a low-pass filter with a relatively high cutoff frequency effectively modulating HR up to 1.0 Hz. The sympathetic cardiac control operates as a low-pass filter with a much lower cutoff frequency. It is capable of modulating heart rate only at frequencies below 0.15 Hz.

A number of studies have been performed that support this finding. It has been tested in dogs that broadband electrical stimulation of the vagus is followed by HR changes with minimal dampening up to at least 0.7 Hz [26,27]. Broadband electrical stimulation of the right stellate ganglion is followed by HR changes with a delay of approximately 2 seconds and a dampening that leads to a minimal response above 0.15 Hz. In addition, studies in dogs and in humans show that when a parasympathetic blockade is performed by atropine, the HR fluctuations above 0.15 Hz are eliminated. The frequencies below 0.15 Hz are partly unaffected. Finally, cardiac sympathetic blockade with propranolol has been used to show a reduction in HR fluctuations below 0.15 Hz, while frequencies above 0.15 Hz are unaffected. Therefore, HR changes above 0.15 Hz seem to be primarily caused by modulation of cardiac vagal efferent activity.

Respiratory fluctuations in HR are most likely to be caused by the parasympathetic efferent pathways. This is understandable since respiration usually occurs at frequencies greater than about 9 breaths per minute (0.15 Hz). These

observations explain the use of respiratory sinus arrhythmia as a measure of cardiac vagal modulation. This can also explain why respiratory sinus arrhythmia does not always accurately reflect only vagal HR modulation. Sympathetic modulation of respiratory-induced HR changes occurs when the respiratory activity is below 0.15 Hz (fewer than 9 breaths per minute).

The correspondence to a single control mechanism is not clear in the LF region. It has been found in animals that HR fluctuations at frequencies below 0.15 Hz are mediated by both the vagal and sympathetic cardiac nerves. In humans, HR powers between 0.03 – 0.15 Hz can be reduced by either sympathetic or parasympathetic pharmacological blockade. Furthermore, HR fluctuations in this region have been shown to be effected by various stimuli such as periodic breathing, hemodynamic instability, and thermoregulation [21]. Therefore, HR spectrum in the LF region is not specifically a sympathetic marker, since there seems to be a vagal influence and dependency on other mechanisms. However, the reliability of the LF region as a sympathetic marker can be enhanced by designing experimental conditions such that the sympathetic condition is sufficiently activated. In our study, we were able to allow for this due to our paradigm which will be explained in the next section.

2.5.2 Interpretation of BPV

The regulation of blood pressure can be described in context with homeostasis. Homeostatis of blood pressure implies that although the blood pressure changes due to external stimulations, it has a tendency to rebound back to a set reference (i.e. the average blood pressure value). Therefore, it is realized that a lot more information can be extracted from the signal aside from looking at the mean blood pressure and the variance.

Analyzing and quantifying the oscillations of the blood pressure signal around this mean value could lead to additional information and enhanced insight into understanding the mechanisms of cardiovascular control.

HF BP power is not substantially modified in patients with denervated donor hearts. This had led to the suggestion that power in this frequency range is mainly caused by the mechanical effects of respiration on the pressure gradients, size and functions of the heart and large thoracic vessels. However, conflicting findings have cropped up recently. It has been now been suggested that HF BP powers are determined by vagally mediated changes in HR and cardiac output. However, it is yet unclear to what extent is the influence of vagal modulation on HF BP powers.

Cardiac autonomic blockades by administration of atropine and propranolol eliminates only a fraction of the BP variability at frequencies below 0.15 Hz. This shows that the autonomic modulation of the HR is not significant in mediating the LF BP powers. Therefore it is suggested that LF BP powers are mainly caused by the fluctuations in the vasomotor tone and the systemic vascular resistance. Laboratory studies have been conducted on humans that show when a stimulus that increases the sympathetic cardiovascular influences (such as head-up tilt) is administered, the BP powers are increased in the LF (0.05-0.15 Hz) region. When a stimulus that reduces the sympathetic influence is used (i.e. sleep, alpha adrenergic blockade), the BP power predictably decreases. Therefore, it can be stated that LF BP powers (0.05 – 0.15 Hz) are a signature of sympathetic vasomotor tone. This is similar to that demonstrated in the same frequency region for HR power, where the LF region was concluded to be a signature of the sympathetic cardiac drive.

2.6 BARORECEPTOR SENSITIVITY (BRS)

The most common method to improve the assessment of the autonomic nervous system through power spectral analysis is to couple the information obtained from the hemodynamic signal with the information derived from physiological models. To this end, we decided to incorporate the baroreceptor sensitivity calculations to further validate our findings. This allowed us to undertake a modeling approach that considers the relationship between two cardiovascular signals that are physiologically. The arterial baroreflex is a key mechanism for blood pressure homeostasis, is clinically relevant as a predictor of cardiovascular mortality, and is physiologically relevant as an indicator of autonomic control. The sensitivity, or gain, of the arterial baroreflex is calculated routinely from the relation of heart rate responses to variations in systemic arterial pressure [16]. The baroreceptor multivariate model allowed us to evaluate the HR reflex using both the time domain and frequency domain approaches. The methodologies of the two approaches are delineated in the next chapter.

2.7 SUMMARY

A survey of literature on IBS and ANS testing helped us to formulate a test paradigm explained in chapter 3.

Chapter 3

INSTRUMENTATION AND EXPERIMENTAL PROTOCOL FOR COLORECTAL DISTENTION

3.1 INTRODUCTION

In this chapter a description of the gastrointestinal stimulation (in the form of colorectal distention) will be presented. The rationale for choosing the protocol will be described. Electrophysiological variables which serve as indicators of autonomic balance will be identified.

3.2 RATIONALE

While indirect stimulation of the ANS in patients with IBS to elicit ANS responses is possible using methods described earlier; a direct stimulation of the GI system is preferable. Towards this end, a review of the literature was performed. It was

noted that consistently accurate markers which correlate ANS indices with subjective symptoms (discomfort and pain) were not available. There was evidence that lowered sensory thresholds to rectal ballon distentions are a reproducible marker of IBS. In a recent article [6], Bouin et al. subjected a large number of patients with IBS and controls to colorectal distention and studied their rectal sensitivity to distention. They found the patients with IBS more sensitive. The sensitivity (in a statistical sense) in patients was as high as 95.8% and the specificity was 71.8%. Therefore, a colorectal distention protocol designed by our collaborators (Astra Zeneca, Molndal, Sweden) was adopted.

3.3 OBJECTIVES

a. To study the ANS response to rectal balloon stimulation in healthy controls. A number of healthy control subjects will be studied for stabilization of instrumentation parameters and protocol.

b. To study the ANS response to rectal balloon stimulation in patients with IBS. Patients will be recruited from the outpatient population of the GI clinic.

3.4. INSTRUMENTATION

The instrumentation designed for the present study consists of three components:

a. Rectal balloon which expands and hold 500 ml. at a pressure of at least 70 mm. Hg. The balloon is manufactured by Astra Zeneca.

b. Barostat: This was designed by Astra Zeneca and was capable of delivering the above pressure with a fail-safe switch, which can be used to stop the study on demand.

c. Data Acquisition System: Electrophysiological and hemodynamic variables such as ECG, blood pressure waveform, respiration were recorded along with the balloon pressure and volume. The barostat was controlled by Pentium 4 computer with a clock speed of 2.1GHz. The ECG amplifier 7910 made by HP was used. Finapres was used to measure non-invasively the blood pressure using a finger-cuff. Respiration was recorded using a strain gage sensor, tied to a belt (which in turn was placed around the chest). The sampling rate for all signals was 500 samples/channel/second.

3.5 EXPERIMENTAL PROTOCOL

Figures 3.1 and 3.2 represent the experimental protocol carried out for this study. The rectal balloon was tested before the study and was ascertained to be free of leaks. The subject was asked to lie on the bed and the balloon was placed in the rectum. A baseline pressure of less than 1 mm Hg. was present in the balloon following insertion and the ECG, blood pressure and respiration were recorded in a supine condition. A ramp distention was then applied with pressure increasing at a rate of 0.5 mmHg/second. During the procedure the subject continuously indicated his/her discomfort and pain level using Electronic Analog Scale. As soon as the subject indicates a 50% discomfort, the barostat stops the inflation and the pressure within the balloon remains same for a further 3 minutes. At the end of 3 minutes, the pressure

drops to baseline values. There is an "Emergency Stop" button to enable the subject to stop the study at any point of choosing and balloon will deflate to 0 mm Hg. immediately.

3.6 SELECTION OF HUMAN SUBJECTS AND PREPARATION FOR STUDY

Healthy controls subjects were identified through a campus advertisement. Initially, younger human subjects of either gender volunteered for the study. Patients with IBS were selected through outpatient clinics of McMaster's GI division. Healthy controls were not on any medication and were normotensive with no history of any pathology. Patients with IBS who may have been on any medication were asked to discontinue any medicines 48 hours before the study. Patients with diabetes, high blood pressure, rhythm disturbances and other heart problems were excluded by the study nurse through a telephone interview. There were 23 male controls, and 12 female controls, the average age was 30 ± 10 years. There were 2 male, and 20 female patients with IBS studied, the average age was 41 ± 12 years.

3.7 EXPERIMENTAL PROCEDURE

The subjects came to the lab at 8 am, having fasted from 11 pm the night before and having taken an enema. The subjects signed a form which was approved by the institutional review board and indicative of informed consent. The subjects rested comfortably on a bed. A physical examination was performed by a qualified physician. The experimental protocol was explained to the subject. Following the insertion of the balloon the experimental procedure as explained in 3.4 was carried out. The study took approximately 60 minutes.

3. 8 SUMMARY

In this chapter, rationale and experimental design for studies on colorectal distention was presented.

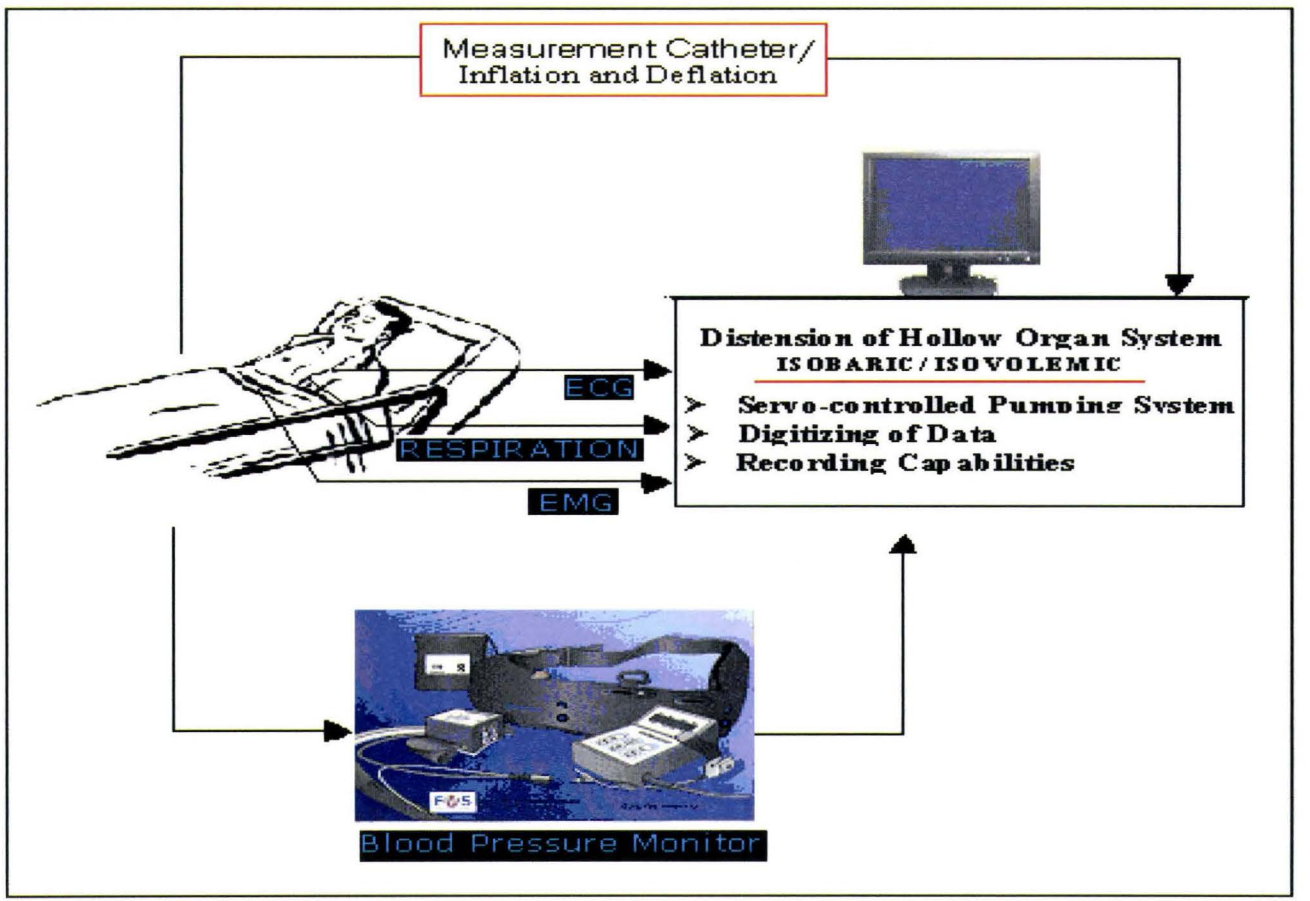

Figure 3.1: Experimental set up for colorectal distention

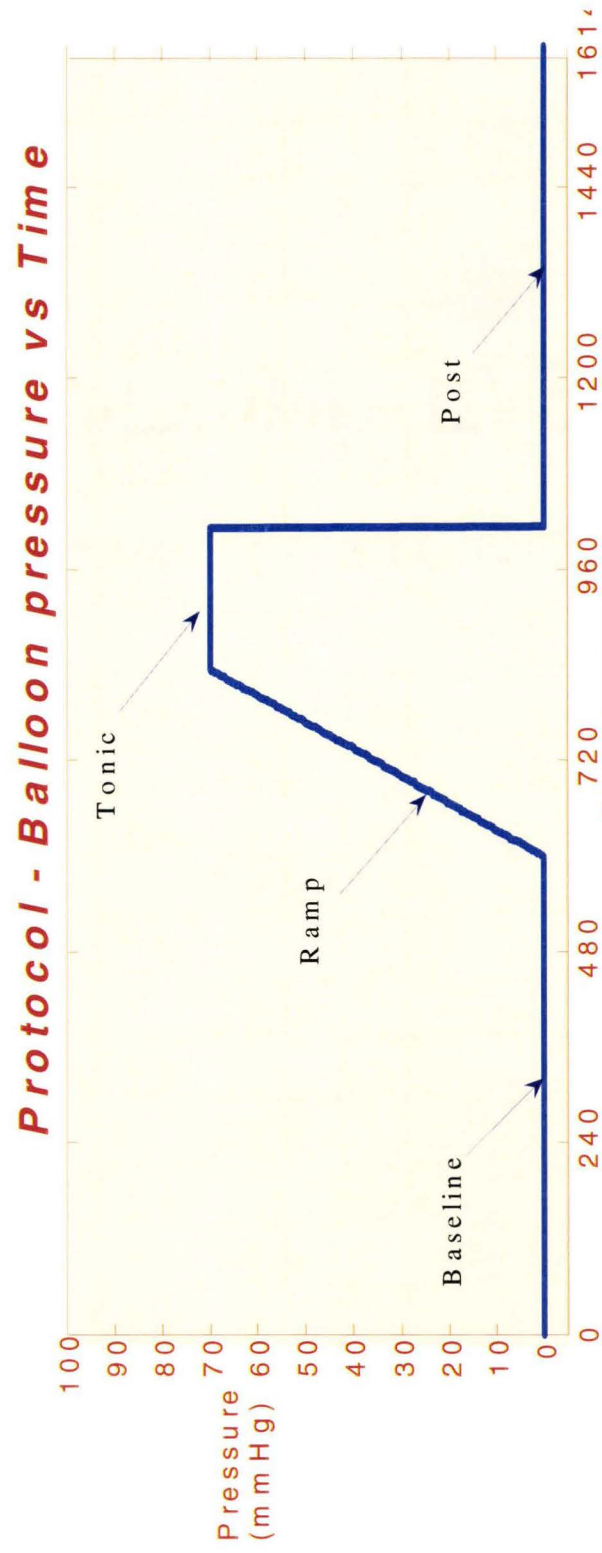

Figure 3.2: Experimental balloon inflation protocol: balloon pressure vs. time.

Chapter 4

DATA ANALYSIS PROCEDURES

4.1 INTRODUCTION

In this thesis, power spectral analysis, time-frequency analysis, and computation of the BRS are the primary methods used for signal processing and quantification of the ANS activity. Initially, stationary and linear techniques were applied to stationary segments of the paradigm. While ramp and post-distension segments of the study were non-stationary, stationary methods were used as a guideline and as a first approximation of the autonomic changes taking place in the nervous system. Techniques employed for the research reported in this thesis were the Blackman Tukey power spectral density (PSD) estimation method, and Autoregressive estimation of the PSD. To obtain continuous estimates, Wigner-Ville decomposition was used as the time-frequency method. This allowed for studying stationary and non-stationary components of the

experiment. For future work, another method, known as Empirical Mode Decomposition (EMD), will be explored to decompose hemodynamic signals into stationary and linear components. The EMD is a novel signal processing procedure, which has recently appeared in the literature.

In addition to obtaining the indices of the ANS through PSD estimation, a unique method was employed for the first time in studying autonomic effects on Gastroenterological (GI) System. Estimation of Baroreceptor Sensitivity (BRS) serves as an indirect measure of the ANS response to external stimulation. It was deemed necessary to validate results obtained from BRS computation using time-domain and frequency-domain procedures. Therefore, three distinct methods of BRS computation described in the literature were employed. In particular, the Three Point Method provided a direct measure of BRS in the time-domain [10,19,21] while Pagani's method and Robbe's algorithm depend on frequency-domain computations.

4.2 METHODS FOR THE COMPUTATION OF THE POWER SPECTRAL DENSITY OF HEMODYNAMIC SIGNALS [10]

In the present study Power Spectral Density estimates were obtained for the heart rate variability (HRV) and the systolic blood pressure variability (SBP) signals.

4.2.1 Estimation of the PSD of the Heart Rate Variability Signal

Following steps are involved in obtaining an estimate of the PSD of the HRV signal

4.2.1.1 QRS Detection [25]

The QRS detection algorithm extracts the R-R intervals from the ECG signal recorded during the study. A robust algorithm is required to perform this task since the ECG signal

is usually contaminated by various types of noise. In addition to the noise, the algorithm must be able to adapt to the inherent physiological variability of QRS complexes. Some of the types of noise and physiological factors that cause variability include: electrode contact noise, power line interference (60Hz), motion artifacts and muscle contractions, baseline drifts and ECG amplitude modulation due to respiration.

There are two types of QRS detectors: Neural network based QRS detection and linear QRS detector. The linear QRS detector consists of the following fundamental processing steps: linear processing, nonlinear transformation, and decision rules for detecting the R-waves. Linear processing typically includes a digital band pass filter, first/second order derivative computation and a moving window integrator. Non linear transformation usually follows the linear transformation and involves the squaring of the amplitude of the ECG signal. This helps in enhancing the difference of magnitude of the QRS periods from the non-QRS periods. Decision rules are a set of criteria that a sample in ECG signal must meet in order to be characterized as a fiducial point on an R-wave. Good decision rules lead to robust QRS detection. The decision rules may consist of several steps that determine the presence of an R-wave such as an adaptive threshold, T-wave discrimination and search-back techniques. A basic method used to locate a QRS complex is to compare the current signal magnitude to a pre-set threshold (usually a percentage of the signal envelope). The adaptive threshold technique utilizes that basic concept but also adjusts the threshold according to the evolving signal envelope and hence compensates the effects of baseline wandering and/or sudden changes in the QRS amplitude. The T-wave discrimination technique makes use of the fact that in ECG signals, there is a physiological refractory period of at least 200 ms between subsequent

QRS complexes. The search-back technique continuously compares the current R-R time interval to the average interval and re-searches a period if the interval is much longer than the average value

The QRS detection algorithm used in the present analysis was based on the work of Ruha [25]. The algorithm is able to achieve good time accuracy in a relatively noisy environment, while at the same time, maintain low computational complexity. The QRS detection algorithm includes a linear digital filtering process and a decision rule. The linear filtering process contains two linear bandpass filters (prefiltering bandpass and bandpass) which aim to attenuate noise and enhance the features used for detection. The decision rule is based on an adaptive amplitude comparison procedure and a T-wave discrimination technique. Since the threshold is continuously adapting to the envelope of the ECG signal, the algorithm is able to capture the dynamic changes that occur during transient physiological states that are present in the present study during colorectal balloon inflation and deflation. The algorithm did not perform a search back.

During the filtering stage, two bandpass filters were used to attenuate the low frequency and high frequency noise. Since we know that the QRS complex contains signal components in the frequency band from 2-100 Hz with a peak at 10-15 Hz, the first band pass filter (0.5-35 Hz) is chosen to filter out the DC component, power line interference, and high frequency noise. A 48^{th} order FIR filter was designed for this purpose. The second bandpass filter designed as a 48^{th} order FIR filter with a passband of 15-40 Hz was chosen to further remove the low frequency motion artifacts (2 to 10 Hz). In addition, utilizing the band 15-40 Hz instead of the 10-35 Hz provides a significant reduction of the T-wave. The orders of the FIR filters were chosen based on

the amplitude response. A comparison of a 12^{th} order, 24^{th} order, and a 48^{th} order FIR filter had revealed much sharper transitions at the 3-dB point. .

The QRS decision rule is then implemented on the filtered ECG signal using an adaptive threshold. The threshold continuously adapts to 40% of the maximum value of the filtered ECG over the previous 2 seconds. If a heart rate of 60 beats/min is assumed, the QRS threshold is arbitrarily set around 60% of the peak value. In reality, the threshold should be set at a lower level (30-40%) in order to decrease the amount of false negatives (missed beats). Such decrease in the false negatives comes at the expense of an increase in false positives that can be corrected more easily than false negatives in the post-processing phase. The threshold level must be adaptive to the varying ECG signal envelopes in order to remain at the same relative level and maintain the desired detection properties. Therefore, after each positive QRS detection, the threshold is raised to 120% of the latest maximum value for 200 ms in order to prevent false detection due to a T-wave.

4.2.1.2 Intermediate Processing of R-R intervals and the HRV Signal

Upon extracting the R-R interval signal from the ECG signal, a conversion of the R-R interval signal to instantaneous heart rate (HR) is performed. The R-R interval is inverted to obtain the instantaneous HR signal. Thereafter, a 2 Hz re-sampling is performed on the HR signal using linear interpolation. Finally, the 0-0.025 Hz frequency component is filtered out as much of the physiologically relevant power in the HR signal lies above 0.025 Hz.

4.2.1.3 Power Spectrum Computation [11]

The power spectrum (PS), also known as the power spectral density, describes the distribution of power over its frequency components. For a uniformly sampled signal x(t), the PS is defined as the mean square value of the signal for each frequency component, over the signals spectra which is the average distribution of power across the frequency range. The computation of the power spectra requires a Fourier Transform (FT) of the signal. The square of the absolute value of the FT represents the power spectrum $P_x(f)$.

$$P_x(f) = X(f)X^*(f) = |X(f)|^2 \tag{4-1}$$

$$X(f) = \int_{-\infty}^{+\infty} x(t)e^{-j2\pi ft}\,dt \tag{4-2}$$

$$x(t) = \frac{1}{2\pi}\int_{-\infty}^{+\infty} X(f)e^{j2\pi ft}\,df \tag{4-3}$$

The estimate obtained by the above mentioned method is a raw estimate of PS and is not generally accepted as a statistically reliable and robust method of computing the power spectrum. Computation of PS for real-life signals requires obtaining a reliable, smooth, and stable estimate. Stable computation of the PS of hemodynamic signals can be obtained by using the following techniques: Blackman Tukey (BT) method, Autoregressive (AR) method.

i) Blackman Tukey Method for computation of the PS of HRV

The Blackman-Tukey method is based on the Weiner-Khinchin relationship, which states that the power spectrum of a signal equals the Fourier Transform (FT) of the autocorrelation function (ACF) of the signal.

$$P_{BT}(f) = \sum_{k=1}^{n} r_{xx}[k]\exp(-j2\pi fk) \qquad -1/2 \leq f \leq 1/2 \qquad (4\text{-}4)$$

The steps used for computing the PS of the HRV signal are as follows. First, the signal detrended and normalized. Upon performing this, the autocorrelation function of the signal is computed. The ACF is then multiplied by a lag window (such as a Bartlett Window) to reduce the variance. The ACF is then truncated to a specific value (0.5 Hz in our case). The FFT of the windowed ACF is computed and a smoothed PS is obtained.

$$P_{BT}(f) = \frac{1}{M} \sum_{k=-m}^{m} w[k]r_{xx}[k]\exp(-j2\pi fk) \qquad (4\text{-}5)$$

ii) Autoregressive Method for PS of HRV

In the autoregressive (AR) approach, the signal x[n] at any instant n, is defined as a linear combination of the past values plus a disturbance [11]:

$$x(n) = -\sum_{k=1}^{p} a(k)x(n-k) + u(n), \quad n = p+1, \ldots, N, \quad N >> p \qquad (4\text{-}6)$$

where a[k], k = 1,2….p are the autoregressive parameters used to describe the process that generates the signal. We can gain more insight into the process that generates the signal by investigating from a digital filter viewpoint. For an all-pole filter with output with x(n) as output and u(n) as a white noise input sequence, the denominator polynomial H(z) of the filter transfer function is defined as

$$H(z) = 1 + \sum_{k=1}^{p} akz^{-k} \tag{4-7}$$

The filter transfer function is 1/H(z). Taking the z-transform of the input-output relationships we get,

$$X(z) = \frac{1}{H(z)} U(z) \tag{4-8}$$

Performing the inverse z- transform and realizing that multiplication in the z-domain amounts to convolution in the time domain, we now get,

$$x(n) = -\sum_{k=1}^{p} a(k)x(n-k) + u(n) \tag{4-9}$$

It is evident that equation (4-6) is the same as the above equation (4-9). Hence, there are two equivalent interpretations for an AR process: (1) The sequence is defined as a linear combination of past values plus a disturbance; (2) The sequence is the output of an all-pole filter, the input of which is excited by white noise.

This process is termed an autoregressive process since the sequence *x(n)* is a linear regression on itself where *u(n)* representing the error. If we move the weighted summation term to left side of Equation (4-6) and perform the z-transform, we get

$$(1 + \sum_{k=1}^{p} a[k]\, z^{-k}) X(z) = U(z) \tag{4-10}$$

Rearranging the terms, we obtain

$$X(z) = \frac{U(z)}{1 + \sum_{k=1}^{p} a[k] z^{-k}} \tag{4-11}$$

and utilizing the relationship between the Fourier-transform and z-transform:

$Z=e^{j2\pi f}$,

$$X(f) = X(e^{j2\pi f}) = \frac{U(j2\pi f)}{1 + \sum_{k=1}^{p} a[k] e^{-j2\pi fk}} \tag{4-12}$$

Since $P_{AR}(f)=|X(f)|^2$ and $U(j2\pi f)$,the power of white noise ***u(n)***, is σ^2 , AR PS

$$P_{AR}(f) = \frac{\sigma^2}{(1 + \sum_{k=1}^{p} a[k] e^{-j2\pi fk})^2} \tag{4-13}$$

In order to calculate the AR PS using Equation (4-13), the coefficients a[*k*] in Equation (4-6) must be solved first. In the following, we first explain the idea of prediction error filter (PEF) then describe the derivation of one solution (Yule-Walker equations) to this

problem from a matrix computation viewpoint [11]. The prediction error filter (PEF) accepts an autoregressive process *x(n)* as an input and outputs the corresponding prediction error *u(n)*. To obtain this filter, we interchange the input and output sequences of the AR generating filter and by inverting the filter transfer function.

The next step is to derive the Yule-Walker equations. Equation (4-6) can be expressed in matrix form as

$$\mathbf{X}_p=\mathbf{X}\mathbf{a}+\mathbf{u} \tag{4-14}$$

Where

$$x_p=\begin{bmatrix} x_{p+1} \\ x_{p+2} \\ . \\ . \\ . \\ . \\ x_N \end{bmatrix} \qquad u=\begin{bmatrix} u_{p+1} \\ u_{p+2} \\ . \\ . \\ . \\ . \\ u_N \end{bmatrix} \qquad a=\begin{bmatrix} -a_1 \\ -a_2 \\ . \\ . \\ . \\ . \\ -a_p \end{bmatrix}$$

$$X=\begin{bmatrix} x_p & \cdots & x_1 \\ x_{p+1} & \cdots & x_2 \\ . & & \\ . & & \\ . & & \\ . & & \\ x_{N-1} & \cdots & x_{N-p} \end{bmatrix}, \quad n=p+1, \ldots, N, \quad N \gg p. \tag{4-15}$$

To solve for the coefficients **a**, the PEF concept is used. For our purposes, we choose the coefficients such that the prediction-error power is minimized. This makes the prediction $x_e(n)$ as close as possible to $x(n)$ in the 2-norm sense. The coefficients $\mathbf{a}_{LS}$ (where the subscript LS stands for least square) is found in such a manner to minimize

$$\left\| x_p - X_a \right\|_2^2 \tag{4-16}$$

and therefore are the solution set to the normal equations:

$$\mathbf{X}^T\mathbf{X}\mathbf{a}_{LS}=\mathbf{X}^T\mathbf{x}_p \tag{4-17}$$

Taking the expectations of both sides of Equation (4-17) we get,

$$E\,(\mathbf{X}^T\mathbf{X})\,\mathbf{a}_{LS}=E\,(\mathbf{X}^T\mathbf{x}_p) \tag{4-18}$$

If {x(n)} is stationary and ergodic, the matrix $E(\mathbf{X}^T\mathbf{X})$ becomes

$$E(X^TX)=\begin{bmatrix} r_{xx}(0) & r_{xx}(-1) & r_{xx}(-2) & \cdots & r_{xx}(-(p-1)) \\ r_{xx}(1) & r_{xx}(0) & r_{xx}(-1) & & \\ r_{xx}(2) & r_{xx}(1) & r_{xx}(1) & r_{xx}(0) & \\ \vdots & & & & \\ r_{xx}(p-1) & & r_{xx}(1) & & r_{xx}(0) \end{bmatrix} = R \tag{4-19}$$

Where $r_{xx}(k)=E[x_{n+k}x_n^*]$ is the autocorrelation function (ACF) of lag k, and **R** is the covariance matrix of {x}. Likewise, from $E(\mathbf{X}^T\mathbf{x}_p)$ in Equation (4-18), we get:

$$E(X^T x_p) = \begin{bmatrix} r_{xx}(1) \\ r_{xx}(2) \\ \\ . \\ . \\ . \\ r_{xx}(p) \end{bmatrix} \equiv r_p \qquad (4\text{-}20)$$

Equation (4-18) is therefore represented as

$$\mathbf{Ra}_{LS} = r_p \qquad (4\text{-}21)$$

Equation (4-21) is the expectation of the normal equations used to determine the coefficients of a stationary AR process. The finite-sample version of Equation (4-21) is referred to as the Yule-Walker equations (4-22)):

$$\begin{bmatrix} r_{xx}(0) & r_{xx}(-1) & \dots & r_{xx}(-(p-1)) \\ r_{xx}(1) & r_{xx}(0) & \dots & r_{xx}(-(p-2)) \\ . & & & . \\ . & & & . \\ . & & & . \\ r_{xx}(p-1) & r_{xx}(p-2) & \dots & r_{xx}(0) \end{bmatrix} \begin{bmatrix} -a_1 \\ -a_2 \\ . \\ . \\ . \\ -a_p \end{bmatrix} = \begin{bmatrix} r_{xx}(1) \\ r_x(2) \\ \\ \\ \\ r_{xx}(p) \end{bmatrix} \qquad (4\text{-}22)$$

From the regression Equation (4-14), we have

$$\sigma^2 = E(u^T u) = E[x_p - X_{aLS})^T (x_p - X_{aLS})]$$

$$= E(x_p{}^t x_p - X_{aLS}{}^T X^T xp + {}_{aLS}{}^T X^T X_{aLS}). \qquad (4\text{-}23)$$

Substituting Equation (4-18) into the above equation and where,

$$E(\mathbf{X}^T\mathbf{x}_p)=\mathbf{r}_p=\mathbf{R}_{aLS}, \tag{4-24}$$

and realizing that $E(\mathbf{x}_p{}^T\mathbf{x}_p)=r_o$, we get

$$\sigma^2 = r_0 - r_p{}^T a_{LS} - a_{LS}{}^T r_p + a_{LS}{}^T r_p$$

$$= r_0 - r_p{}^T a_{LS} \tag{4-25}$$

Combining Equation (4-21 and (4-25) together into one matrix equation as follows:

$$\begin{bmatrix} r_{xx}(0) & r_{xx}(-1) \dots & r_{xx}(-p) \\ r_{xx}(1) & r_{xx}(0) \dots & r_{xx}(-(p-1)) \\ . & & . \\ . & & . \\ . & & . \\ r_{xx}(p) & r_{xx}(p-1) \dots & r_{xx}(0) \end{bmatrix} \begin{bmatrix} 1 \\ -a_1 \\ . \\ . \\ . \\ -a_p \end{bmatrix} = \begin{bmatrix} \sigma^2 \\ 0 \\ . \\ . \\ . \\ 0 \end{bmatrix} \tag{4-26}$$

where the first row is given by Equation (4-25) and the remaining rows are given by Equation (4-21) with a new first column coming from the right side of the equation. These equations are called forward prediction-error equations. By varying the forward prediction-error equations, we obtain backward prediction-error equations as

$$\begin{bmatrix} r_{xx}(0) & r_{xx}(-1) \dots & r_{xx}(-p) \\ r_{xx}(1) & r_{xx}(0) \dots & r_{xx}(-(p-1)) \\ . & & . \\ . & & . \\ . & & . \\ r_{xx}(p) & r_{xx}(p-1) \dots & r_{xx}(0) \end{bmatrix} \begin{bmatrix} a_p \\ . \\ . \\ . \\ a_1 \\ 1 \end{bmatrix} = \begin{bmatrix} 0 \\ . \\ . \\ . \\ 0 \\ \sigma^2 \end{bmatrix} \tag{4-27}$$

Equations (4-26) and (4-27) can be solved jointly using the Levinson-Durbin recursion (LDR), which requires only $\mathbf{O}(\mathbf{n}^2)$ flops comparing to $\mathbf{O}(\mathbf{n}^3)$ of Gaussian

elimination method. The idea of Levinson-Durbin recursion is to start with a simple system of equations. Then by induction we use that result to solve a 2*2 system, and recursively iterate until the solution to a p*p system is obtained. In summary, the Levinson-Durbin algorithm recursively computes the parameter sets $\{\mathbf{a}_1(\mathbf{1}), \sigma_1^2\}$, $\{\mathbf{a}_2(\mathbf{1}), \mathbf{a}_2(\mathbf{2}), \sigma_2^2\}, \ldots, \{\mathbf{a}_p(\mathbf{1}), \mathbf{a}_p(\mathbf{2}), \ldots, \mathbf{a}_p(\mathbf{p}), \sigma_p^2\}$, **the** final set at order p is the desired solution of the Yule-Walker equations. The recursive algorithm is initiated by

$$a_1(1) = \frac{r_{xx}(1)}{r_{xx}(0)} \tag{4-28}$$

$$\sigma_1^{\,2} = \left(1 - |a_1(1)|^2\right) r_{xx}(0) \tag{4-29}$$

with the recursion for k= 2,3, …, p given by

$$a_k(k) = -\frac{r_{xx}(k) + \sum_{l=1}^{k-1} a_{k-1}(l)\, r_{xx}(k-l)}{\sigma_{k-1}^2} \tag{4-30}$$

$$a_k(i) = a_{k-1}(i) + a_k(k)\, a_{k-1}^*(k-i), \quad i = 1, 2, \ldots, k-1 \tag{4-31}$$

$$\sigma_k^2 = (1 - |a_k(k)|^2)\sigma_{k-1}^2 \tag{4-32}$$

The form of the algorithm given in Equations 4-30 to 4-32 is due to Levinson (9, 11), who formulated an efficient means for solving a hermitian Toeplitz set of equations, and to Durbin (9, 11), who refined the algorithm to take advantage of the special form of the right-hand-side vector

One of the difficulties while computing the PS using the AR method is that the model order, p, which describes the signal, is not predefined. For the HRV time series recorded during various physiological conditions, the statistical properties of the signal may differ. Hence, there is no single model order that uniformly describes HRV signals recorded from these diverse sources. Changing the model order across different physiological conditions and/or patients may introduce a new variable into the computation of PS. A number of criteria are defined in the literature to assist the selection of the model order [11]. In this thesis we chose a model order between 12-14. This number is supported by Akaike information criterion (AIC) using six sets of HRV data from healthy subjects (three male and three female with an average age of 24±1 years) during both supine and standing condition. The AIC is defined as [11]:

$$\mathrm{AIC}(k) = N \ln \rho k + 2k \qquad (4\text{-}33)$$

Where N is the data record length, ρk is the estimate of the white noise variance (prediction error power) for the kth order AR model.

4.2.1.4 Comparison between Autoregressive Modeling & Blackman-Tukey Method

The AR PS usually has higher resolution than BT PS. It is due to an implicit extension of the measured ACF [11]. Assume that an AR PS is desired and that the

known ACF samples are $\{\mathbf{r}_{xx}(0), \mathbf{r}_{xx}(1),\ldots, \mathbf{r}_{xx}(p)\}$. The AR coefficients are found by substituting the known ACF samples into the Yule-Walker equations and solving. Then the AR PS as defined on the z-plane is

$$P_{AR,\,e}(z) = \frac{\sigma_e^{\,2}}{A_e(z)A_e^{\,*}(1/z^{*})} = \sum_{k=-\infty}^{\infty} r_{xx,\,e}(k)\, z^{-k} \tag{4-34}$$

where the subscript "e" denotes the estimates quantities. It can be shown that the implied ACF $\mathbf{r}_{xx,e}(\boldsymbol{k})$, which is given by the inverse z-transform of $\mathbf{P}_{AR,e}$, is

$$r_{xx,\,e}(k) = \begin{cases} r_{xx}(k) & for\ 0 \le k \le p \\ -\sum_{l=1}^{p} a_e(l)\, r_{xx,\,e}(k-1) & for\ k \rangle p \end{cases} \tag{4-35}$$

Hence the estimate of the ACF matches the known ACF up to lag $\boldsymbol{p}$ and the remaining samples are extrapolated by a recursive difference equation. In contrast to AR method, the BT procedure windows the known ACF sequence and then extrapolates the sequence by appending zeros, thus giving rise to the usual smearing of the spectral estimator. The AR spectral estimator extrapolates the autocorrelation sequence according to Equation (4-35). Consequently, the resultant spectral estimate is a less biased version of the true one. In summary, when the AR modeling assumption is valid, AR PS is less biased and has a lower variability than BT PS [11].

4.2.1.5 Frequency Bands and their physiological Relevance

It is stated in literature that there are three major frequency bands in the power spectrum in human subjects as well as in unconscious, anesthetized dogs [9]. A low-frequency (LF) peak that appears within the spectral band ranging from 0.06 to 0.15 Hz is associated with baroreceptor-mediated blood pressure control and believed to contain mainly a sympathetic component [5,9]. A high frequency (HF) peak in the range 0.15 to 0.5 Hz is strongly correlated with parasympathetically mediated respiratory sinus arrhythmia. A very-low-frequency (VLF) peak below 0.05 Hz has been linked with vasomotor control and/or temperature control. In the current study, the very-low-frequency band is removed before the calculation of PS because the frequency resolution in this band is poor and its huge peak usually obscures the study of the other two (LF & HF) bands.

The LF power, calculated by a summation of the power under the PS curve between 0.06 Hz to 0.15 Hz, is an index of the sympathetic modulation of the heart. On the other hand, the HF power, calculated by the same method but between 0.15 to 0.5 Hz band, reflects the modulation of the parasympathetic (or vagal) modulation of the heart. Finally the LF:HF ratio, the ratio between LF power, is an index of the balance between sympathetic and parasympathetic modulation of the sinus node.

4.2.2 TIME-FREQUENCY ESTIMATION of HRV, SBPV

4.2.2.1 Background

The usefulness of time-frequency distribution (TFD) in medicine is based on the nonstationary nature of most physiological signals. Signals recorded from human subjects are a function of a number of biological variables. For example, physiological

conditions such as exercise, and postural changes do not satisfy the criteria for stationarity, a basic assumption while computing power spectra using traditional methods such as Blackman-Tukey (BT) algorithm or autoregressive (AR) procedure [9]. New techniques from the class of time-frequency distributions include Wigner-Ville distribution (WVD) wavelet transform (WT), SHORT-TIME Fourier transform (STFT) may prove to be more relevant while dealing with nonstationary signals. Among these methods, Wigner-Ville distribution provides the most accurate estimate with the highest frequency resolution [5]. The smoothed Wigner-Ville distribution has been demonstrated to be a good estimation method for short nonstationary time series [5]. Its resolution is enhanced by independent time and frequency smoothing using a moving N-event data window [5]. This chapter describes Wigner-Ville distribution and its implementation for analyzing the HRV signal.

Time-frequency distributions map a one-dimensional signal into a two-dimensional function of time and frequency. They are conceptually similar to a musical score with time running along one axis and frequency running along the other axis. The time-frequency plane gives an indication of which spectral components are present at any time instant. Hence this technique permits one to understand and describe situations elegantly where the frequency content of a signal is changing with time.

The time-frequency distributions of a signal can be divided into two main classes: linear and quadratic time-frequency distributions. A fundamental difference in the classes is the signal order utilized in the integrals. For the linear distribution, an integral of first order signal terms is used, while for quadratic method an integral of second order terms is computed. From a signal processing point of view, a linear time-frequency

distribution means that if a signal is a linear combination of some frequency components, its time-linearity is a desirable property in any application involving multi-component signals. Unfortunately the most commonly used linear method STFT has a crucial drawback, i.e., there is tradeoff between time and frequency resolutions. A longer window length gives better frequency resolution but poorer time resolution, while a shorter window length gives better time resolution but poorer frequency resolution. Unfortunately, both time and frequency resolutions cannot be improved simultaneously.

On the contrary, the quadratic methods do not satisfy the property of linearity but are able to improve the time and frequency resolutions simultaneously. This group of methods includes the Wigner-Ville distribution (ED), and the reduced interference distribution (RID).

The following is an example of the non-linear property WVD. Assume $x(t)$ contains two sinusoids of frequency $f_1 f_2$ as:

$$x(t) = A_1 \exp(j2\pi f_1 t) + A_2 \exp(j2\pi f_2 t), \qquad F_2 \geq F_1 \tag{4-36}$$

The WVD is then:

$$W_f(t,f) = 2\pi A_1^2 \delta(f - f_1) + 2\pi A_2^2 \delta(f - f_2) + 4\pi A_1 A_2 \cos(2\pi(f_2 - f_1)t)\delta(f - \frac{1}{2}f_1 + f_2)), \quad F_2 \geq F_1 \tag{4-37}$$

where $\delta(f-f_i)$is an impulse centered at $f = f_i$. It can be seen that the WVD of a two component signal contains not only the addition of the WVD of two single-component signals but also an extra term whose frequency lies in the middle of the two original frequency components. The extra item is called cross-term. It makes the interpretation of WVD difficult. However, equation (4-37) also reveals that the amplitude of the cross-term is oscillating along time, which suggests we might use time smoothing to remove the cross-term.

4.2.2.2 Wigner-Ville Distribution

The concept of WVD was introduced by Wigner in the field of physics and incorporated into signal analysis. A general definition of the continuous WVD of any complex function $z(t)$is given by:

$$W_z(t,f) = \int_{-\infty}^{-\infty} z(t+\tau/2)\, z^*(t-\tau/2)\, e^{-j2\pi f\tau} d\tau \qquad (4\text{-}38)$$

where t is the time domain variable and f is the frequency variable. The * denotes the complex conjugate. This estimator is sometimes referred to as the Wigner distribution (WD) if $z(t)$ is a real function. The WVD yields high resolution in both time and frequency and has several nice properties, including preservation of time and frequency support, instantaneous frequency, group delay, etc.

The main drawback of the WVD is that it produces cross-terms (or interference) if the signal contains more than one frequency component due to its quadratic nature (equation 4-37). Besides, the WVD is generally not fully positive for the total range of time and frequency, which obscures its physical interpretation. We can minimize these problems as follows: a) we can use an analytic signal instead of real signal to suppress cross-terms between positive and negative frequencies and b) we can perform time and frequency smoothing to suppress regions where spectra are negative and also reduce cross-terms.

4.2.2.3 Necessity and Calculation of Analytic Signal

In most practical cases, the signals to be analyzed consist only of real values. In these cases it is necessary to form the corresponding analytic signal. To see the importance of using the analytic signal, consider the Wigner distribution (WD) defined by:

$$W_x(t, f,) = \int_{-\infty}^{+\infty} x(t+\tau/2)\, x^*(t-\tau/2)\, e^{-j2\pi f \tau} d\tau \qquad (4\text{-}39)$$

where x(t) is the real signal to be analyzed. This distribution differs from the Wigner-Ville distribution (equation 4-38) by its use of the real signal, x(t), instead of the analytic signal, z(t). The relationship between the Wigner distribution and Wigner-Ville distribution is:

$$W_x(t,f) = \frac{1}{4}[W_z(t,f) + W_z(t,-f)] + \gamma(t,f) \tag{4-40}$$

where γ((t,f) represents the cross-terms between positive and negative frequencies and is oscillatory in nature.

The analytic signal z(n) corresponding to x(n) is defined in the discrete time domain as:

$$z(n) = x(n) + jH[x(n)] \tag{4-41}$$

where H[x(n)] represents the Hilbert transform of x(n). Alternatively, the analytic signal can be defined in the frequency domain as:

$$Z(f) = \begin{cases} 2X(f), & 0<f<1/2 \\ X(f), & F = 0 \\ 0, & -1/2<F<0. \end{cases} \tag{4-42}$$

There are two main methods to obtain an analytic signal from a real world and in our case, a physiological signal. A direct method is to use its frequency definition: a signal with no negative frequency components. That is, form the Fourier transform of the signal, set the negative frequency values to zero, and perform the inverse Fourier transform. Another method is to use a Hilbert transform filter to produce the required complex component of the signal, which when added to the real part produces the desired analytic signal as given by equation (4-41). Hilbert transform filter has the ideal impulse response given in equation 4-43.

$$h(n) = \begin{cases} \dfrac{2\sin^2(\pi n/2)}{\pi n} & = for\ n \neq 0 \\ 0, & = for\ n = 0 \end{cases} \tag{4-43}$$

4.2.2.4 Time and Frequency Smoothing

As mentioned previously, in order to suppress negative regions and cross-terms it is necessary to apply smoothing in the time and frequency domain. Theoretically the smoothing process is a 2-D convolution of the WVD with a function G(*t,f*) given by:

$$W(t,f) = \frac{1}{2\pi} \int_{-\infty}^{+\infty} \int_{-\infty}^{+\infty} W(\tau, \xi) G(t-\tau, f-\xi) d\tau d\xi \tag{4-44}$$

It is shown that using G(*t,f*) as defined below can help the situation:

$$G(t,f) = \frac{1}{T\Omega} e^{\frac{-t^2}{T^2}} e^{\frac{4f^2}{\Omega^2}} \tag{4-45}$$

With TΩ, equation (4-44) yields a positive WVD. Here, T and Ω define the amount of smear in the time and frequency domains respectively. Such a smoothed WVD has no cross-terms and no negative regions. The price paid is a smear in the time and frequency domain and a loss in the phase information. However, partially smoothed WVD has proved to be a very useful tool.

Large computational savings can be achieved by computing the smoothed WVD directly, rather than computing the WVD and then performing a 2-D convolution. In analog form, the smoothed WVD is given directly by:

$$W_z(t,f) = \int_{-\infty}^{+\infty} |h(\tau/2)|^2 \int_{-\infty}^{+\infty} z(t+\tau/2-\tau') z^*(t-\tau/2-\tau') g(\tau') d\tau' e^{-j2\pi f\tau} d\tau \tag{4-46}$$

where *t* is the time variable and *f* is the frequency variable, $g(\tau')$ and $h(\tau/2)$ are the time and frequency smoothing window respectively. For discrete signals, the smoothed WVD is given by:

$$W_{zz}(n,m)=\frac{1}{2}N\sum_{k=0}^{N-1}|h(k)|^2\sum_{p=-m+1}^{m-1}g(p)z(n+p+k)x^*(n+p-k)e^{-2i\pi km/N} \qquad (4\text{-}47)$$

where n is the time index, m is the frequency index, g(p) and h(k) are time and frequency smoothing windows respectively. M is the parameter defining the time smoothing window width and N is the time window over which a spectral estimation is calculated.

4.2.2.5 Choice of the Smoothing Windows

In order to use equation 4-47 to produce the smoothed Wigner-Ville distribution of a given signal, we must decide the window shape and corresponding parameters. For our specific application, a rectangular time window g(p) with length 2M+1 (M=9) and a Gaussian frequency window h(k) with length N(N=127) have been chosen. Note first that the length of the time window g(p), 2M+1, is much shorter than N in this case. Also the time window g(p) is centered at the actual time index, n, (equation 4-47, p=-M, ...,+M). Therefore this smoothing method is able to provide a good time resolution. The Gaussian frequency window h(k) is given by:

$$h(k)=e^{-1/2[\alpha k/(N/2)]^2} \qquad 0 \le |k| \le N/2 \qquad (4\text{-}48)$$

$$2.5 \le \alpha \le 3.5$$

With these parameters, it has been possible to generate reliable estimates of time-frequency distributions that follow the signal structure particularly well under

nonstationary conditions. Moreover, they allow a better evaluation of the frequency content of transitory periods that cannot be obtained otherwise.

4.3 BARORECEPTOR SENSITIVITY COMPUTATION

There are several ways to assess the baroreceptor sensitivity (BRS). However, there is one general dichotomy that defines the different methods – invasive and non-invasive. It may be determined invasively from the cardiovascular response to certain drugs or it can be determined using non-invasive techniques that use raw blood pressure and RR-interval signals. Predominant invasive methods described in the literature are nitroprusside infusion and phenylephrine infusion. The two commonly employed non-invasive method depend on finding monotonically increasing sequence of BP and RR intervals or computation of the cross-spectra of the two hemodynamic signals.

4.3.1 Sequence Method [7,10,16]

The sequence method is one of the non-invasive methods used to determine the BRS. It involves cycling through a data set that contains the beat to beat RR interval and the blood pressure (systolic) values. The concept involves finding sequences of three or more beats whereby the blood pressure and RR interval increase concomitantly or decrease concomitantly. Depending on the stress paradigm used, a threshold value is used for the systolic blood pressure. For example for an extremely strenuous situation an additional criterion for selecting the increasing or decreasing RR interval and systolic blood pressure would involve only selecting systolic blood pressure values that are increasing or decreasing by at least 3 mm Hg or more. The least squares method is used

to approximate a best-fit line for each of these sequences of simultaneously increasing or decreasing RR intervals and systolic blood pressures. A correlation coefficient was computed between two signals. Those slopes between instantaneous values of BP and RR where the correlation was 0.8 or greater were used as a measure of the BRS. The slopes for each of these sequences are averaged to arrive at an average value of baroreceptor sensitivity

4.3.2 Robbes' Cospectral Method [16]

Robbes' Method involves analysis of the spectrum of the blood pressure and the R-R interval signal. The spectrum of the systolic (or diastolic) blood pressure and the R-R interval signal is obtained using the FFT. The coherence function of the two signals in the sympathetic nervous system range of 0.04 – 0.15 Hz is further analyzed. For regions where the coherence is greater than 0.5, the mean value of the transfer function of the blood pressure signal to the R-R interval is calculated.

$$BRS = \left| \frac{P_{xy}(f)}{P_{xx}(f)} \right| \left(msec/mmHG \right), \quad where\ coherence = \frac{P_{xy}^2}{(P_{xx} \cdot P_{yy})} > 0.5, \quad for\ 0.04\ Hz < f < 0.50\ Hz \tag{4-49}$$

This value is representative of the BRS for the subject.

4.3.3 Pagani's Transfer function Method [16]

The Pagani Method of computing the BRS is similar to the Robbes' method. However, there are two fundamental differences. Firstly, the region of interest is from 0.04 – 0.15 (sympathetic region) and 0.15 – 0.5 Hz (parasympathetic region). Secondly, the transfer function is computed as the autospectra of the R-R interval divided by the cross spectra of the blood pressure and R-R interval.

$$BRS = \left| \frac{RRint(f)}{SBP(f)} \right| \left(msec/mmHg \right), \quad where\ coherence = \frac{P_{xy}^2}{(P_{xx} \cdot P_{yy})} > 0.5,$$
$$for\ 0.04\ Hz < f < 0.50\ Hz \qquad (4\text{-}50)$$

The value of the BRS is still determined as the mean of the transfer function over the frequency bands defined above where the coherence is equal to greater than 0.5.

4.4 SUMMARY

In this chapter various methods of determining parameters from HRV and BPV for quantifying ANS are explained in detail.

Chapter 5

RESULTS

5.1 INTRODUCTION

In this chapter results of investigations into gastrointestinal stimulation of healthy subjects and patients with IBS will be presented. Quantitative measures that describe the autonomic nervous system provide useful information to better identify patients with IBS.

5.2 BASIC HEMODYNAMIC VARIABLES

Results of colorectal distention on basic hemodynamic variables are shown in Tables 5.1, 5.2.

	Baseline	Ramp	Tonic	Post
Systolic Blood Pressure (mm. Hg)	†122.49 ± 6.21*	†129.33 ± 17.34	†142.78 ± 17.52	†130.48 ± 15.35
Diastolic Blood Pressure (mm. Hg)	†67.40 ± 11.56*	†71.17 ± 11.50	†80.70 ± 12.00	†72.92 ± 11.91
Heart Rate (Bts/min)	65.64 ± 16.21*	68.15 ± 8.31	70.86 ± 9.59	64.88 ± 7.64

Table 5.1: Mean Heart Rate and Blood Pressure of Control Subjects (n =35). *: $p<0.05$ cf. to ramp, tonic, post. †: $p<0.05$ cf. to patients.

	Baseline	Ramp	Tonic	Post
Systolic Blood Pressure (mm. Hg.)	133.57 ± 1.30*	141.94 ± 22.18	160.55 ± 26.06	144.42 ± 21.90
Diastolic Blood Pressure (mm. Hg.)	73.30 ± 14.83*	78.70 ± 14.88	89.89 ± 17.27	80.22 ± 14.08
Heart Rate (Bts./min.)	64.14 ± 8.68 **	67.35 ± 9.10	70.09 ± 10.86	63.90 ± 8.23

Table 5.2: Mean Heart rate and Blood Pressure values for patients with IBS (n = 22).*: $p<0.05$ cf. ramp, tonic and post. **: $p<0.05$ cf. ramp and tonic

The colorectal distention caused significant increases in the heart rate, blood pressure (both systolic and diastolic components) in healthy controls and patients, as can be seen from tables 5.1 and 5.2. Also, patients differed from controls significantly.

5.3 COMPARISON OF METHODS

Three different methods were applied to the heart rate and blood pressure data to compute the baroreceptor sensitivity: sequence method, Pagani's (transfer function) method, and Robbes' (cross spectral) method. The BRS values used for comparison were determined for systolic blood pressure in the controls group. Outliers were identified as

being more than two standard deviations away from the mean. Paired t-test were performed between baseline-ramp, baseline-post distension and between tonic-post phases of the study. The statistical significance level was set to $p<0.05$.

5.3.1 Comparisons within the healthy control group during the balloon distention

The sequence method was applied to both the controls' and patients' group. For the controls group, during the 20-minute baseline, the mean UP-BRS was 11.86 ± 4.37 mm/Hg. During the ramp phase the mean UP-BRS dropped to 10.63 ± 6.23 ms/mmHg. During the tonic state, it dropped slightly to 10.28 ± 4.44 ms/mmHg. Finally during the 20 minute post state, the UP-BRS value rebounded to 11.88 ± 5.08 ms/mmHg.

The down-BRS followed a similar pattern. The results of the 35 healthy controls can be seen in Table 5.3. The distention (tonic state) decreased the BRS significantly in healthy controls ($p<0.05$).

The Pagani's (transfer function) method was applied to the hemodynamic data obtained during baseline, tonic and post- distention states. The signal was deemed to be linear during these states because the balloon pressure, the independent variable was stable during these periods. The values for the baseline tonic and post-distention states were 10.96±4.68 ms/mmHg, 10.18± 5.64 ms/mmHg, 10.80 ± 5.53 ms/mmHg respectively. Table 5.5 shows the table of results as well as the significance values.

The third technique used was based on performing the cross-spectral analysis of the heart rate signal and blood pressure signal (Robbes' Method). The BRS values obtained for this method was baseline, tonic and post-distention states were 15.77± 6.83 ms/mmHg, 15.14 ± 4.83ms/mmHg, 16.62± 6.04 ms/mmHg respectively (Table 5.7). The method permitted identification of distension state ($p<0.05$).

5.3.2 Comparisons within the patient group during the balloon distention

Hemodynamic data obtained from patients with IBS was processed using the sequence method and the BRS trend was assessed during baseline, ramp, tonic and post states (Table 5.4). During the 20 minute baseline, the mean UP-BRS value was 10.00± 5.13 ms/mmHg. This value dropped to 6.71± 3.14 ms/mmHg during the ramp phase. The UP-BRS value remained suppressed during the 3 minute tonic phase where the balloon pressure was held constant. The mean UP-BRS during that phase was 8.14±3.30. The twenty minute post phase showed a mean UP-BRS value of 9.80± 5.30, slight rebound to baseline values. The DOWN-BRS revealed a similar pattern as the UP-BRS. The patients showed a drop in the UP-BRS level during the ramp and tonic phase compared to the baseline values.

It is evident from the statistical results that the BRS changes significantly during the ramp and tonic states for both UP-BRS and DOWN-BRS. In addition the change in BRS value was significant for ramp vs. post-distention for DOWN-BRS and tonic vs post-distention for UP-BRS.

Pagani's transfer function and Robbe's cross-spectral methods of BRS computation did not always show significance (Tables 5.6, 5.8). However, both Robbe's cross-spectral method and Pagani's transfer function method of BRS computation did show that there was a prevalent trend - similar to that observe with the sequence method. These two methods also showed that the BRS value dropped in the tonic state and rebounded in the post state. These results show that the sequence method is more sensitive for picking up baroreceptor reflex incidences than the cross-spectral or transfer function method.

5.3.3 Comparison between the controls' and the patients' group during the balloon distention

For both UP-BRS and DOWN-BRS values for the patients group, the trend was similar to that of the controls group. There was suppression in the mean BRS values during the ramp and tonic states with a rebound to close to baseline during the post phase. However, the BRS was lower for patients as compared to controls. This shows that the baroreceptor sensors of the patients group are less sensitive and less responsive to fluctuations during distention then the healthy controls. These trends were also observed in using Robbe's cross-spectral and Pagani's transfer function methods (statistical significance is provided in the tables).

5.3.4 Summary

Based on these results, one can observe that the sequence method provides an excellent comparison of BRS values between the three physiological states. Not only can individual activation of BRS for each state be computed, but both UP-BRS and DOWN-BRS can be determined. Finally, estimation through averaging is inherent in Pagani's transfer function Method and Robbe's cross spectral method for computing the BRS, thereby smearing the BRS sensitivity computations. From the results obtained and trends shown, a physiological hypothesis can be made. Since the BRS computed was that with a vagal efferent, it can be hypothesized that the vagal components of the ANS are impaired for patients.

	BRS (Sequence Method) - Control Group							
	EVENT: --->	BASELINE		RAMP		TONIC		POST	
	subject #	Brs Up*	Brs Down*	†Brs Up	Brs Down	Brs Up	†Brs Down	Brs Up	Brs Down
1	exp214001	-	-	7.90	5.25	5.83	4.77	6.84	7.63
2	exp214003	10.43	6.52	2.75	3.37	7.89	4.09	7.37	4.65
3	exp214004	12.42	9.91	22.67	13.61	15.78	11.72	15.31	5.55
4	exp214005	14.21	12.25	-	-	-	32.57	14.15	26.68
5	exp214006	7.51	11.29	8.88	14.24	7.94	9.14	8.41	9.38
6	exp214007	9.80	12.66	11.77	9.30	5.22	9.33	10.26	14.15
7	exp214008	6.60	9.86	12.89	13.86	8.88	16.85	13.36	7.27
8	exp214009	12.10	12.73	15.08	11.92	19.29	12.46	8.62	13.14
9	exp214011	9.13	10.78	5.16	10.96	9.53	5.03	11.62	10.99
10	exp214012	11.34	7.91	6.55	5.80	-	6.49	11.02	-
11	exp214013	12.64	9.23	13.87	11.96	10.46	12.60	13.13	-
12	exp214020	8.13	15.21	6.24	13.09	8.59	13.58	6.82	11.41
13	exp214026	15.01	14.36	5.15	15.58	10.78	3.17	8.13	14.39
14	exp214028	5.32	3.75	3.82	-	5.37	5.98	5.97	5.61
15	exp214030	12.57	8.95	-	-	16.35	10.84	14.81	10.44
16	exp214031	34.43	15.61	21.60	13.01	14.73	4.69	27.24	16.76
17	exp214032	19.98	12.82	15.44	10.36	12.27	9.80	13.03	9.75
18	exp214033	8.41	6.80	4.85	1.45	5.76	3.57	8.63	11.06
19	exp214040	18.71	19.08	17.94	19.34	16.62	20.64	19.92	17.62
20	exp214041	11.09	14.67	3.19	10.46	5.38	10.91	30.22	15.14
21	exp214045	36.65	23.88	-	9.26	43.01	24.52	30.69	23.05
22	exp214047	17.15	18.35	8.34	5.10	5.20	5.52	22.83	16.15
23	exp214048	16.59	8.23	56.59	8.63	4.47	16.40	20.81	9.37
24	exp214049	17.90	19.18	14.88	11.43	14.12	13.60	-	-
25	exp214050	14.93	14.98	17.54	22.79	12.19	8.62	-	22.33
26	exp214058	3.00	2.19	1.97	2.15	1.44	1.28	2.11	2.05
27	exp214062	5.82	3.99	-	-	-	-	-	2.25
28	exp214065	17.41	19.70	22.04	16.45	16.74	13.98	20.25	20.94
29	exp214066	18.82	15.16	19.28	-	17.64	25.44	19.18	16.69
30	exp214067	9.08	11.07	14.92	9.51	10.66	7.89	9.93	9.66
31	exp214075	12.14	9.09	7.95	6.35	6.01	15.51	12.73	9.94
32	exp214077	14.18	11.16	9.07	10.82	11.20	8.55	14.60	13.29
33	exp214078	7.65	3.73	6.22	3.11	10.75	2.17	7.10	4.06
34	exp214080	10.28	9.56	3.92	5.02	4.74	6.05	8.19	7.04
35	exp214084	9.08	8.19	6.95	2.54	7.96	8.01	9.42	8.45
	Mean:	11.86	11.18	10.63	9.89	10.28	9.14	11.88	11.30
	St. Dev:	4.37	4.61	6.24	10.25	4.44	4.78	5.09	5.52

Table 5.3: Sequence Method of Computing the Baroreceptor Sensitivity (ms/mmHg). Highlighted values are outliers. *:$p<0.05$ cf. tonic. †: $p<0.05$ cf. patients.

BRS (SEQUENCE METHOD) - Patient Group									
	EVENT: --->	BASELINE		RAMP		TONIC		POST	
	subject #	Brs up*	Brs down*	Brs up	Brs down**	Brs up **	Brs down	Brs up	Brs down
1	exp114016	10.21	13.01	12.05	11.62	10.41	12.53	10.99	11.44
2	exp114021	5.16	4.40	5.02	4.20	4.34	7.24	5.76	5.18
3	exp114022	9.23	11.93	7.20	10.54	7.84	9.86	-	-
4	exp114023	7.91	10.18	5.13	8.75	9.61	8.54	16.58	10.09
5	exp114024	-	6.82	3.76	8.79	-	12.01	-	-
6	exp114029	3.25	7.73	2.79	4.88	-	4.03	2.17	8.06
7	exp114034	5.51	5.02	6.32	3.59	1.97	3.32	4.44	4.80
8	exp114036	12.37	5.23	-	-	5.76	7.80	-	-
9	exp114037	21.65	19.21	5.19	-	11.15	3.40	18.47	10.12
10	exp114039	12.36	11.71	13.45	16.72	15.59	-	13.60	15.44
11	exp114043	8.10	10.05	9.12	7.94	4.02	7.98	9.94	12.39
12	exp114052	6.01	8.93	2.65	3.65	-	-	5.02	9.81
13	exp114053	7.31	5.18	5.82	6.04	7.49	3.67	4.97	5.07
14	exp114055	10.50	14.40	4.17	7.60	8.41	5.19	11.25	13.25
15	exp114056	12.40	13.71	22.36	6.15	7.21	1.60	-	-
16	exp114059	8.31	7.10	6.17	5.57	-	2.73	-	-
17	exp114063	46.89	26.29	8.32	12.87	17.57	30.68	38.23	34.09
18	exp114064	21.85	23.82	7.79	20.84	8.87	-	-	-
19	exp114071	4.58	6.52	3.31	4.33	4.61	8.16	4.70	5.39
20	exp114073	10.87	9.42	6.06	4.84	11.50	6.22	-	-
21	exp114076	10.45	11.18	10.27	7.87	5.16	5.30	14.76	11.28
22	exp114081	10.33	10.44	8.26	7.33	6.18	5.13	10.58	10.16
	MEAN:	**10.00**	**10.63**	**6.71**	**8.24**	**8.14**	**6.56**	**9.80**	**9.54**
	STD DEV.:	5.13	4.80	3.14	4.61	3.30	3.31	5.30	3.15

Table 5.4: Sequence method of computing the baroreceptor sensitivity for patients group (ms/mmHg). Highlighted BRS values are outliers, highlighted subjects are diarrhea patients, all of which were omitted from calculation). *:$p < 0.05$ cf. Ramp, Tonic. **:$p<0.05$ cf. to Post.

	BRS (Transfer Function Method) Control Group			
	subject #	BASELINE	†TONIC	POST
1	exp214001	48	6.01	4.27
2	exp214003	6.52	5.88	5.68
3	exp214004	6.26	21.92	12.12
4	exp214005	7.66	7.69	7.09
5	exp214006	8.38	6.66	8.96
6	exp214007	13.53	8.47	11.87
7	exp214008	12.12	6.44	8.72
8	exp214009	7.42	11.13	8.47
9	exp214011	7.6	8.27	8.7
10	exp214012	8.67	7.12	6.01
11	exp214013	9.86	11.98	11.52
12	exp214020	11.34	6.57	8.47
13	exp214026	15.01	11.66	13.5
14	exp214028	5.35	4.4	5.44
15	exp214030	9.65	8.81	9.75
16	exp214031	20.44	22.24	15.35
17	exp214032	12.88	9.39	10.64
18	exp214033	9.15	4.29	8.6
19	exp214040	17.88	18.92	18.07
20	exp214041	18.15	19.81	20.77
21	exp214045	39.41	44.54	-
22	exp214047	15.83	6.71	24.7
23	exp214048	14.28	18.49	10.48
24	exp214049	15.3	12.98	11.9
25	exp214050	20.94	12.6	47.64
26	exp214058	1.62	0.49	2.23
27	exp214062	7.6	1.76	3.71
28	exp214065	14.26	19.49	17.35
29	exp214066	26.5	28.67	25.6
30	exp214067	8.45	8.77	7.82
31	exp214075	9.91	14.48	11.15
32	exp214077	14.52	7.48	14.31
33	exp214078	6.12	6.28	8.83
34	exp214080	7.23	5.39	6.58
35	exp214084	6.93	3.71	7.66
	MEAN:	10.96	10.18	10.80
	STDEV:	4.68	5.64	5.53

Table 5.5: Method based on transfer function: BRS results for Controls data (ms/mmHg). Highlighted BRS values are outliers. †: $p<0.05$ cf. patients.

BRS (Transfer Function Method) Patient Group				
	subject #	BASELINE	TONIC	POST
1	exp114016	8.52	6.83	10.05
2	exp114021	4.68	5.08	5.52
3	exp114022	9.81	9.12	10.99
4	exp114023	4.29	12.91	12.44
5	exp114024	8.71	8.15	8.5
6	exp114029	3.93	2.97	2.59
7	exp114034	5.23	1.65	-
8	exp114036	6.94	6.34	4.36
9	exp114037	20.44	7.84	12.95
10	exp114039	11.42	11.76	14.06
11	exp114043	6.06	5.31	9.05
12	exp114052	5.59	4.44	7.64
13	exp114053	3.34	5.54	3.78
14	exp114055	20.34	5	12.84
15	exp114056	12.02	9.81	48
16	exp114059	6.36	2.54	3.64
17	exp114063	84.77	16.86	63.48
18	exp114064	21.52	12.4	9.93
19	exp114071	5.59	4.29	4.87
20	exp114073	6.53	4.94	-
21	exp114076	7.74	15.81	7.92
22	exp114081	8.22	5.35	10.83
	MEAN:	8.60	7.51	8.42
	STDEV:	5.12	3.76	3.53

Table 5.6: Method based on transfer function: BRS results for Patient data (ms/mmHg). Highlighted patients belong to diarrhea group and highlighted values are outliers.

	BRS (Cross Spectral Method) - Control Group			
	subject #	BASELINE	†TONIC*	†POST
1	exp214001	11.06	9.24	12.8
2	exp214003	12.66	10.07	16.15
3	exp214004	7.21	22.38	-
4	exp214005	12.86	15.58	14.97
5	exp214006	13.23	11.59	13.14
6	exp214007	28.76	18.87	22.11
7	exp214008	15.32	12.51	14.95
8	exp214009	16.41	16.27	20.26
9	exp214011	11.18	16.11	17.49
10	exp214012	16.18	11.63	13.41
11	exp214013	13.57	16.9	15.02
12	exp214020	8.64	10.78	8.33
13	exp214026	21.22	20.89	19.06
14	exp214028	5.16	8.88	6.58
15	exp214030	16.24	13.99	30.87
16	exp214031	32.3	28.1	23.67
17	exp214032	23.08	16.51	14.08
18	exp214033	14.03	10.39	12.72
19	exp214040	30.7	20.1	24.48
20	exp214041	27.92	19.25	21.44
21	exp214045	25.32	21.5	25.2
22	exp214047	29.51	12.3	25.91
23	exp214048	10.17	20.51	13.81
24	exp214049	22.98	21.55	20.29
25	exp214050	23.45	23.76	81.47
26	exp214058	3.84	2.43	4.57
27	exp214062	5.78	6.18	4.92
28	exp214065	36.98	21.67	26.49
29	exp214066	40.71	30	45.23
30	exp214067	13.21	13.63	13.18
31	exp214075	14.37	17.8	21.6
32	exp214077	15.7	12.38	15.89
33	exp214078	17.75	10.91	12.28
34	exp214080	18.07	10.57	16.28
35	exp214084	13.88	9.63	24.01
	MEAN:	15.77	15.14	16.62
	ST. DEV:	6.83	4.83	6.04

Table 5.7: BRS of Controls group using Robbe's cross-spectral method (ms/mmHg). Highlighted values are outliers. Highlighted values are outliers. *: $p<0.05$ cf. baseline and post. †: $p<0.05$ cf. patients.

BRS (Cross Spectral Method) - Patient Group				
	subject #	BASELINE	TONIC	POST
1	exp114016	8.31	11.82	9.7
2	exp114021	11.4	15.89	11.12
3	exp114022	13.33	12.04	13.81
4	exp114023	16.08	14.6	26.7
5	exp114024	10.14	16.6	14.59
6	exp114029	10.34	5.99	4.1
7	**exp114034**	**11**	**3.69**	**6.19**
8	**exp114036**	**13.99**	**9.23**	**19.04**
9	exp114037	40.77	14.18	20.02
10	exp114039	33.98	15.43	15.84
11	exp114043	14.22	8.08	13.37
12	exp114052	10.13	7.77	11.3
13	exp114053	9.26	10.17	9.96
14	**exp114055**	**17.89**	**14.79**	**25.89**
15	exp114056	13.64	10.46	5.15
16	exp114059	12.29	5.37	7.69
17	**exp114063**	**36.85**	**32.06**	**39.21**
18	exp114064	23.14	17.96	7
19	exp114071	11.42	11.22	8.99
20	exp114073	9.37	10.13	-
21	exp114076	17.81	16.97	15.61
22	exp114081	12.7	11.2	16.8
	MEAN:	12.72	11.99	12.46
	STDEV:	3.78	3.79	5.66

Table 5.8: BRS of patient group computed using Robbe's cross-spectral method (ms/mmHg). The highlighted patients are from the diarrhea group and the highlighted BRS values are outliers.

5.4 RESULTS OF COMPUTING THE POWER SPECTRA OF HRV AND BPV IN HEALTHY CONTROLS AND PATIENTS

Autoregressive and Blackman Tukey algorithms were used to estimate the power spectrum of the heart rate variability signal and the systolic blood pressure variability.

5.4.1 Results of Autoregressive Power Spectral Computations for Controls and Patients: HRV

For the controls group, results showed that there were no significant changes in power spectral parameters except for the suppression of the HF area from baseline to post-distention state (Table 5.9). In the patient's group there was a significant increase in the LF:HF ratio from baseline state to tonic state (1.00 ± 0.35 in baseline to 1.12 ± 0.33 in tonic state). In addition, there was significant drop in HF power from baseline state to tonic state (Table 5.10).

The trends observed from the results suggest a sympathetic increase from baseline to tonic and also a vagal withdrawal. The LF power increase is higher in patients as compared to the controls group. This may also suggest a sympathetic overdrive for the patients.

5.4.2 Results of Blackman Tukey Power Spectra Computation for Controls and Patients: HRV

The controls' group showed a significant increase in the LF:HF ratio from the baseline state to the tonic state. There was also a significant suppression of the HF power in the tonic state when compared to the baseline state. The HF power was also significantly suppressed in the post-distention state when compared to the baseline state.

The increase in the LF:HF ratio from baseline state to post-distention state was significant as well (Table 5.11).

The patients' group did not reveal any significance except for the significant drop in HF power from baseline state to tonic state (Table 5.12). This suppression of HF power was similar to that realized in the controls group between the tonic and baseline states. However, the patients' group showed a trend towards a greater suppression of the HF power than the controls' group and greater increase in the LF power. This may suggest once again a sympathetic overdrive and a vagal impairment in the patients group.

Results of Power Spectral Analysis of HRV from Controls: AR Method										
		BASELINE			TONIC			POST		
	SUBJECT ID.	LF	HF*	LF:HF RATIO	LF	HF	LF:HF RATIO	LF	HF	LF:HF RATIO
1	214001	-	-	-	4973.41	2491.65	2.00	4732.44	1895.88	2.50
2	214003	6404.84	5837.61	1.12	7036.64	5198.12	1.35	6416.61	4576.79	1.40
3	214004	5762.91	6434.93	0.90	3841.77	7441.89	0.52	3999.28	4031.44	0.99
4	214005	5103.51	5772.143	0.88	4144.86	5381.74	0.77	3947.53	4155.09	0.95
5	214006	6945.66	4371.53	1.63	5226.93	4619.17	1.13	6857.82	3087.338	2.28
6	214007	6066.63	4056.97	1.59	5850.49	6577.56	0.89	6041.93	5090.9	1.19
7	214008	4554.81	4416.14	1.03	5450.08	6754.65	0.81	4430.43	4661.39	0.95
8	214009	5596.69	6839.07	0.86	6340.19	5796.11	1.09	6861.50	5996.33	1.14
9	214011	4763.87	6411.67	0.75	7122.77	5241.61	1.36	4399.73	4256.96	1.03
10	214012	5766.84	5222.17	1.11	4507.26	6225.15	0.72	5263.24	6280.05	0.84
11	214013	4380.01	7544.17	0.59	5153.54	7192.92	0.72	4015.40	4955.14	0.81
12	214020	4832.35	6015.82	0.81	6207.78	4938.02	1.26	5184.40	6184.21	0.84
13	214026	5044.94	6348.00	0.79	6771.37	7268.87	0.93	5006.92	5589.86	0.90
14	214028	5631.41	6320.36	0.93	7892.60	4491.95	1.76	5071.46	6341.91	0.84
15	214030	4948.95	5975.24	0.83	5991.50	6521.40	0.92	5215.18	6619.95	0.80
16	214031	7464.05	9038.59	0.83	3882.95	7200.11	0.54	5422.26	7313.78	0.77
17	214032	6130.52	4932.55	1.27	4378.30	3885.66	1.13	4572.62	2899.30	1.58
18	214033	5587.83	5391.04	1.16	7418.60	4082.80	1.82	4712.96	6519.44	0.74
19	214040	4898.30	6129.79	0.80	4601.84	6535.67	0.70	4821.86	5524.26	0.89
20	214041	5407.89	8175.05	0.66	3937.41	8980.86	0.44	5195.35	5826.88	0.90
21	214045	3478.13	7495.35	0.48	3299.90	9091.28	0.36	5138.37	6929.20	0.75
22	214047	7253.93	5299.89	1.37	4848.55	5464.57	0.89	4683.05	6861.09	0.70
23	214048	4674.76	6793.49	0.67	4377.66	6564.10	0.67	4273.62	6874.28	0.63
24	214049	5172.49	6774.16	0.77	5233.15	7330.08	0.71	4440.35	6894.25	0.69
25	214050	5798.99	5885.16	1.00	5547.53	4823.25	1.15	5569.96	6874.36	0.81
26	214058	6070.24	4328.50	1.48	5535.71	3123.47	1.77	6573.29	4021.69	1.66
27	214062	2989.25	5885.10	0.50	-	-	-	-	-	-
28	214065	4348.65	5325.12	0.83	6352.15	5983.38	1.06	4849.77	7068.35	0.73
29	214066	5352.58	6420.81	0.85	5309.30	5493.66	0.97	5017.08	6487.50	0.77
30	214067	5482.51	5296.45	1.04	6075.93	4179.78	1.45	6116.82	3718.06	1.71
31	214075	5448.28	7000.04	0.79	3869.04	6877.45	0.56	5734.86	6212.63	0.92
32	214077	4637.73	5655.33	0.82	4262.67	6891.44	0.62	7260.37	5072.80	1.43
33	214078	5239.75	6203.43	0.85	6263.42	6149.25	1.02	6077.61	5889.41	1.09
34	214080	5998.75	4263.35	1.42	8124.52	4139.18	1.96	7448.40	4208.20	1.77
35	214084	4957.97	5345.67	0.93	6436.88	5168.38	1.25	6144.50	5739.76	1.25
	Mean:	5358.71	5976.61	0.95	5478.43	5826.62	1.04	5338.15	5431.13	1.10
	ST Dev:	929.80	1118.32	0.29	1242.83	1499.84	0.44	949.80	1366.86	0.45

Table 5.9: Results of power spectral analysis of HRV from controls group using AR method (ms^2/Hz). *: $p<0.05$ cf. post.

Results of Power Spectral Analysis of HRV from Patients: AR Method										
		BASELINE			TONIC			POST		
	SUBJECT ID.	LF	HF*	LF:HF RATIO*	LF	HF	LF:HF RATIO	LF	HF	LF:HF RATIO
1	114016	5044.35	7020.10	0.73	5111.81	4836.92	1.06	3935.38	6697.62	0.59
2	114021	6274.00	3819.89	1.66	6996.43	5536.58	1.26	-	-	-
3	114022	4181.52	6506.31	0.64	5020.57	6629.15	0.76	4933.82	6614.14	0.83
4	114023	5366.62	5999.46	0.89	5130.39	7025.05	0.73	5023.82	6051.22	0.83
5	114024	4283.82	6137.57	0.73	7309.08	6073.36	1.20	6028.46	6148.42	1.03
6	114029	4572.29	5492.05	0.84	4916.14	3542.58	1.39	5272.05	2927.58	1.80
7										
8										
9	114037	5811.31	6431.21	0.90	6874.43	6219.02	1.11	6372.02	6452.14	0.99
10	114039	4460.44	5411.86	0.84	5082.10	7125.64	0.71	4851.61	5742.99	0.85
11	114043	4866.62	6264.14	0.77	6606.18	6004.16	1.10	4600.11	5812.35	0.81
12	114052	5211.51	5055.56	1.06	3721.52	6178.21	0.60	6676.67	4442.68	1.51
13	114053	6176.25	3610.14	1.76	6121.67	3925.94	1.56	6537.39	3517.85	1.89
14										
15	114056	4760.18	6631.29	0.72	4620.72	3706.27	1.25	-	-	-
16	114059	7217.78	4603.43	1.63	-	-	-	-	-	-
17										
18	114064	4937.60	7928.82	0.63	4890.03	4347.64	1.12	-	-	-
19	114071	5436.63	5633.25	0.98	5906.17	5549.08	1.06	-	-	-
20	114073	5963.77	5354.36	1.11	4169.65	3781.36	1.10	-	-	-
21	114076	4643.10	4666.57	1.07	8738.34	4519.47	1.93	4059.35	5165.81	0.89
22	114081	5396.83	5038.40	1.07	5801.55	5625.78	1.03	4018.94	4850.88	0.85
	Mean:	5255.81	5644.69	1.00	5706.87	5330.95	1.12	5192.468	5368.64	1.07
	S. Dev:	794.36	1100.34	0.35	1278.11	1187.08	0.33	995.9939	1223.01	0.42

Table 5.10: Results of power spectral analysis of HRV from the patient group using AR method (ms^2/Hz). The highlighted subjects were from the diarrhea group and were excluded from statistics. *: $p<0.05$ cf. tonic.

Results of Power Spectral Analysis of HRV from Controls: BT Method											
		BASELINE			TONIC			POST			
	SUBJECT ID.	†LF	HF*	LF:HF RATIO*	LF	HF	LF:HF RATIO	LF	HF	LF:HF RATIO	
1	214001	-	-	-	116.32	11.15	10.43	-	-	-	
2	214003	83.98	41.93	2.05	106.46	20.73	5.14	79.67	46.28	1.73	
3	214004	74.54	49.56	1.50	43.15	80.04	0.54	-	-	-	
4	214005	72.59	53.06	1.57	80.75	45.83	1.76	-	-	-	
5	214006	194.86	60.13	3.48	177.09	77.88	2.27	204.54	48.33	4.34	
6	214007	201.69	51.61	5.11	154.01	95.99	1.60	189.35	64.85	2.92	
7	214008	-	-	-	67.50	58.97	1.14	-	-	-	
8	214009	132.58	117.24	1.16	173.01	78.57	2.20	183.47	69.68	2.63	
9	214011	61.97	64.42	0.98	96.97	30.12	3.22	93.58	33.43	3.32	
10	214012	165.20	88.27	1.91	135.74	116.43	1.17	113.30	139.68	0.81	
11	214013	106.84	142.08	0.76	146.85	106.57	1.38	177.40	74.37	2.39	
12	214020	107.31	145.66	0.76	194.85	59.20	3.29	120.46	131.76	0.96	
13	214026	135.68	114.09	1.25	153.33	99.76	1.54	151.36	99.47	1.60	
14	214028	124.02	125.01	1.01	207.14	46.94	4.41	128.80	119.37	1.22	
15	214030	128.59	124.36	1.12	144.25	109.09	1.32	122.38	129.74	0.98	
16	214031	124.17	128.92	1.02	107.53	144.75	0.74	120.68	131.93	0.94	
17	214032	186.76	67.60	2.86	85.10	42.15	2.02	102.01	25.45	4.01	
18	214033	142.07	109.60	1.66	210.14	43.39	4.84	126.70	124.30	1.07	
19	214040	119.29	134.75	0.92	131.71	123.02	1.07	148.94	105.13	1.52	
20	214041	116.72	125.37	0.93	59.92	122.32	0.49	162.45	91.06	1.82	
21	214045	84.41	167.22	0.56	42.94	207.58	0.21	113.78	138.43	0.94	
22	214047	153.41	97.46	1.75	177.21	76.13	2.33	130.03	119.84	1.16	
23	214048	125.07	126.49	1.08	96.52	154.36	0.63	118.56	129.82	0.98	
24	214049	126.77	123.26	1.05	106.93	144.71	0.74	123.08	127.47	1.13	
25	214050	129.97	123.78	1.07	158.45	95.29	1.66	138.73	115.13	1.20	
26	214058	202.32	49.65	4.26	221.80	24.98	8.88	201.49	50.30	4.66	
27	214062	48.91	196.99	0.26	-	-	-	-	-	-	
28	214065	78.91	47.44	2.08	45.89	80.90	0.57	70.47	55.60	1.39	
29	214066	134.48	118.31	1.17	154.56	98.23	1.57	125.34	127.97	1.01	
30	214067	152.42	101.11	1.58	207.94	46.34	4.49	208.85	45.64	4.76	
31	214075	111.42	130.27	0.95	111.25	125.46	0.89	138.40	103.10	1.37	
32	214077	122.61	131.53	0.96	118.60	134.81	0.88	150.19	104.16	1.58	
33	214078	128.18	122.37	1.07	158.87	94.41	1.68	152.72	98.85	1.71	
34	214080	188.02	65.12	3.04	211.97	42.82	4.95	212.56	42.37	5.08	
35	214084	166.89	86.61	1.98	191.46	61.71	3.10	179.52	72.66	2.64	
	Mean:	121.35	108.83	1.35	133.07	89.52	2.00	142.96	92.21	2.06	
	ST Dev:	34.88	36.95	0.67	51.67	42.15	1.44	37.99	36.25	1.31	

Table 5.11: Results of power spectral analysis of HRV from controls group using BT method (ms^2/Hz). Highlighted values were omitted as outliers. *: $p<0.05$ cf. tonic and post. †: $p<0.05$ cf. to patients.

Results of Power Spectral Analysis of HRV from Patients: BT Method										
		BASELINE			TONIC			POST		
	SUBJECT ID.	LF	HF*	LF:HF RATIO	LF	HF	LF:HF RATIO	LF	HF	LF:HF RATIO
1	114016	131.06	120.57	1.19	191.78	59.88	3.20	93.05	155.47	0.62
2	114021	210.80	44.02	5.37	176.77	77.57	2.28	201.67	52.89	4.36
3	114022	112.03	138.73	0.85	131.00	122.52	1.07	97.18	153.33	0.73
4	114023	143.80	109.60	1.38	156.02	96.21	1.62	140.78	112.03	1.27
5	114024	107.28	141.08	0.85	172.78	77.09	2.24	150.37	100.08	1.97
6	114029	116.57	137.81	0.90	101.48	25.79	3.93	99.10	28.64	3.46
7										
8										
9	114037	138.93	112.76	1.26	167.44	85.77	1.95	158.54	92.70	1.82
10	114039	125.34	127.41	1.03	83.77	164.90	0.51	153.89	99.56	1.70
11	114043	98.89	154.26	0.67	183.44	69.13	2.65	115.73	137.13	0.87
12	114052	156.97	97.17	1.74	121.82	129.80	0.94	178.42	76.18	2.41
13	114053	210.81	43.94	4.88	206.34	48.25	4.28	216.21	38.41	5.85
14										
15	114056	123.72	127.99	1.00	87.25	39.70	2.20	-	-	-
16	114059	194.09	60.18	3.63	-	-	-	-	-	-
17										
18	114064	106.89	143.00	0.78	-	-	-	-	-	-
19	114071	131.11	121.99	1.14	180.71	70.74	2.55	-	-	-
20	114073	138.62	112.97	1.29	75.30	50.51	1.49	-	-	-
21	114076	172.37	81.52	3.02	207.70	47.11	4.41	136.78	116.00	2.50
22	114081	158.02	96.39	1.67	175.17	79.10	2.21	118.27	136.02	0.93
	Mean:	143.18	109.52	1.81	151.17	77.75	2.35	143.08	99.88	2.19
	ST.Dev	34.53	33.32	1.43	44.66	36.38	1.15	39.15	41.56	1.56

Table 5.12: Results of power spectral analysis of HRV from the patient group using the BT method (ms^2/Hz). Highlighted subjects were from diarrhea group and excluded from statistics.*: $p<0.05$ cf. tonic.

5.4.3 Results of Autoregressive Power Spectra Computations for Controls and Patients: SBPV

The power spectrum results of the systolic blood pressure using the autoregressive method did not show significance for the patient group (Table 5.14). However for the controls group, the HF power increased significantly from the baseline state to the tonic state. As a result the LF:HF ratio decreased significantly from the baseline state value of 1.27 ± 0.28 to the tonic state value of 1.13 ± 0.29 (Table 5.13). In addition, the HF power dropped significantly from the tonic state to the post-distention. As a result, the LF:HF ratio increased significantly from the tonic state value of 1.13 ± 0.29 to 1.31 ± 0.34 in the post-distention state (Table 5.13). When comparing the controls group to the patient group, the patients showed a trend of being less sympathetic and more vagal. This was antipodal to what we observed using HRV power spectrum and BRS computations.

5.4.4 Results of Blackman Tukey Power Spectra Computations for Controls and Patients: SBPV

The Blackman Tukey method of power spectral analysis applied to the systolic blood pressure revealed significant results in the patient group. The LF power dropped significantly from the baseline state to the tonic state. In addition, the LF:HF ratio increased significantly from the tonic state to the post state (Table 5.15). The patients' group did not reveal results of statistical significance (Table 5.16). When comparing the controls group to the patient group, there were no LF power trends. However, the patients did show a trend for a higher HF power. This was antipodal to the results obtained using other methods.

These results show that different methods of computing power spectra do not yield similar results for SBPV power spectra.

Results of Power Spectral Analysis of SBPV from Controls: AR Method										
		BASELINE			TONIC			POST		
	SUBJECT ID.	LF	HF	LF:HF RATIO	LF	HF*	LF:HF RATIO*	LF	HF	LF:HF RATIO
1	214001	-	-	-	5634.93	3752.11	1.50	4406.16	2480.31	1.78
2	214003	7352.09	4302.35	1.72	7110.73	5635.21	1.26	6171.31	5362.41	1.18
3	214004	6070.30	3804.51	1.60	6561.73	5333.88	1.23	5710.33	3561.16	1.60
4	214005	6780.21	5443.42	1.28	7361.81	3955.49	1.86	5699.11	3300.93	1.73
5	214006	6198.74	4639.41	1.35	6358.21	4807.50	1.32	6239.89	4497.03	1.39
6	214007	6580.08	3983.01	1.68	6358.21	4807.50	1.32	6362.95	5327.77	1.19
7	214008	5453.69	3382.59	1.61	5004.95	5216.41	0.96	6096.41	2956.59	2.06
8	214009	6879.69	5059.65	1.37	6055.89	6166.01	0.98	5138.31	5844.10	0.88
9	214011	6843.36	3791.44	1.81	6274.06	5016.71	1.25	6584.97	4059.80	1.62
10	214012	7040.96	4586.56	1.57	6084.44	5772.46	1.05	6593.67	5086.93	1.30
11	214013	6053.82	5278.72	1.16	5565.19	5670.95	0.98	6434.18	4632.92	1.39
12	214020	5452.42	3938.15	1.39	7559.49	4621.82	1.64	6316.65	4235.62	1.50
13	214026	6221.49	5544.52	1.14	6586.94	5212.66	1.26	6350.03	5310.10	1.21
14	214028	6468.79	4832.09	1.37	7202.78	3247.92	2.22	5791.68	5270.35	1.12
15	214030	5469.00	5269.98	1.05	7023.18	5167.39	1.36	6429.41	5100.15	1.27
16	214031	6278.81	3940.89	1.61	6939.97	4243.09	1.64	7102.98	3773.29	1.90
17	214032	6115.35	5537.65	1.11	3527.62	3210.72	1.10	4790.17	2766.06	1.73
18	214033	5224.88	6232.44	0.84	7097.75	5570.25	1.27	5020.26	6784.88	0.76
19	214040	6206.15	4607.43	1.34	5671.37	5771.76	0.98	6128.05	5044.16	1.22
20	214041	6628.87	4642.98	1.48	4800.01	8298.70	0.58	6052.43	3222.62	1.95
21	214045	6290.27	5169.82	1.28	6366.33	6783.15	0.94	6134.79	4961.18	1.28
22	214047	6140.55	5321.77	1.15	5388.91	5918.91	0.91	6103.17	4453.19	1.33
23	214048	6531.58	4294.58	1.60	6848.06	5575.18	1.23	5468.05	5442.10	1.02
24	214049	5883.48	6088.30	0.96	5806.17	8086.49	0.72	5349.51	7098.62	0.75
25	214050	6079.67	5564.66	1.09	7074.99	5348.00	1.32	6177.48	5280.73	1.17
26	214058	6063.64	5498.71	1.12	4796.92	6707.39	0.72	6113.03	4674.56	1.35
27	214062	4708.19	6584.45	0.72	-	-	-	-	-	-
28	214065	6161.44	4475.15	1.39	6375.92	5611.52	1.14	6499.77	4705.99	1.38
29	214066	6202.11	5626.22	1.13	5509.86	5466.59	1.01	5611.24	5811.30	0.99
30	214067	5518.52	4974.33	1.11	6651.82	6670.02	1.00	6158.90	4534.71	1.37
31	214075	5785.84	5099.74	1.13	4537.89	5658.36	0.80	6507.67	5132.75	1.27
32	214077	6517.61	4876.69	1.37	5203.63	6931.35	0.75	6391.19	5364.18	1.20
33	214078	4837.75	6613.16	0.74	6245.29	6502.25	0.96	5279.32	7613.07	0.70
34	214080	5487.64	5800.62	0.96	6197.84	7460.05	0.83	6062.26	5544.64	1.09
35	214084	5251.06	6284.46	0.85	6279.61	4412.18	1.42	6159.70	6441.21	0.98
	Mean:	6081.71	5032.07	1.27	6086.66	5617.03	1.13	5983.38	4872.81	1.31
	St. Dev:	610.70	830.95	0.28	901.50	1146.13	0.29	572.97	1182.78	0.34

Table 5.13: Results of power spectral analysis of SBPV from controls group using AR method ($mmHg^2/Hz$). *: $p<0.05$ cf. baseline, post.

	Results of Power Spectral Analysis of SBPV from Patients: AR Method									
		BASELINE			TONIC			POST		
	SUBJECT ID.	LF	HF	LF:HF RATIO	LF	HF	LF:HF RATIO	LF	HF	LF:HF RATIO
1	114016	6437.62	4108.50	1.57	7307.11	3992.40	1.83	6058.67	3921.68	1.64
2	114021	6483.35	4836.41	1.37	6508.11	6351.59	1.02	6358.86	5851.05	1.14
3	114022	6006.19	5959.20	1.02	6565.15	5110.94	1.28	6487.56	6037.87	1.09
4	114023	6119.57	6238.92	0.98	5462.40	3475.90	1.57	5790.15	5832.54	1.00
5	114024	5930.72	6855.34	0.87	5143.06	7432.02	0.69	6047.59	5300.85	1.14
6	114029	4572.29	5492.05	0.84	4916.14	3542.58	1.39	5272.05	2927.58	1.80
7	114034	5752.85	4769.71	1.25	5410.93	4008.94	1.35	5453.25	5185.09	1.07
8	114036	4941.73	5041.57	0.98	5486.99	4814.29	1.14	6557.44	4664.83	1.41
9	114037	6501.95	5618.63	1.15	6176.04	5853.79	1.06	6673.51	5283.78	1.32
10	114039	5630.20	4302.07	1.33	6013.69	6198.84	0.97	6522.13	4205.45	1.58
11	114043	5107.98	6745.05	0.77	4953.68	5940.04	0.83	5326.41	6184.53	0.89
12	114052	5338.37	5725.58	0.94	3565.67	7831.15	0.46	5680.92	5669.92	1.04
13	114053	6302.07	3722.02	1.81	6737.54	5347.68	1.26	6637.93	3331.85	2.17
14	114055	5563.69	5064.95	1.11	5605.53	7223.75	0.78	5461.31	5269.31	1.07
15	114056	5888.43	4831.04	1.22	5116.82	3327.84	1.54	-	-	-
16	114059	5958.67	4438.27	1.36	-	-	-	-	-	-
17	114063	4468.25	7240.69	0.62	3367.11	8768.25	0.38	4358.73	7511.33	0.59
18	114064	5954.85	5950.46	1.02	5552.79	3159.64	1.76	-	-	-
19	114071	5817.92	5714.55	1.03	5500.13	5447.79	1.01	6627.51	4901.51	1.38
20	114073	4117.47	5601.59	0.77	4471.98	6171.70	0.72	-	-	-
21	114076	5850.28	4846.93	1.26	7428.05	6554.34	1.13	4986.97	5279.46	0.94
22	114081	5889.60	3821.52	1.56	5476.16	5083.68	1.08	5863.84	5464.43	1.09
	Mean:	5772.64	5267.12	1.16	5699.68	5342.47	1.15	6023.86	5013.75	1.30
	St.Dev:	1875.67	1852.33	0.34	2034.81	2155.54	0.41	2121.89	1960.52	0.40

Table 5.14: Results of power spectral analysis of SBPV from patient group using AR method ($mmHg^2/Hz$). None of the results were significant, $p>0.05$. Highlighted patients were from the diarrhea group and were not included in the statistics.

Results of Power Spectral Analysis of SBPV from Controls: BT Method

		BASELINE			TONIC			POST		
	SUBJECT ID.	LF	†HF	LF:HF RATIO	LF	HF	LF:HF RATIO	LF	HF	LF:HF RATIO
1	214001	-	-	-	99.23	24.50	4.07	-	-	-
2	214003	95.02	30.51	3.41	65.58	58.09	1.13	90.80	33.23	2.99
3	214004	111.60	16.08	7.16	91.25	34.98	2.66	-	-	-
4	214005	95.28	30.05	3.81	97.17	29.32	3.31	-	-	-
5	214006	201.74	50.60	4.65	198.00	52.23	3.79	219.81	33.20	6.62
6	214007	213.51	38.63	6.11	168.50	82.09	2.05	189.45	62.94	3.01
7	214008	-	-	-	93.97	31.99	2.95	-	-	-
8	214009	183.34	67.60	2.84	166.79	75.54	2.21	161.34	90.83	1.78
9	214011	108.29	18.78	6.18	93.07	31.67	2.94	106.81	19.72	5.78
10	214012	191.19	61.08	3.48	181.55	63.31	2.87	197.54	51.56	3.83
11	214013	179.50	69.35	3.06	189.76	60.99	3.11	191.63	58.01	3.30
12	214020	207.59	46.33	4.65	216.68	37.56	5.77	207.08	46.47	4.53
13	214026	181.51	68.89	2.77	196.98	54.62	3.61	186.04	64.30	3.00
14	214028	189.00	63.13	3.13	222.30	32.45	6.85	180.14	71.66	2.81
15	214030	174.15	78.90	2.36	177.82	75.70	2.35	197.97	55.97	3.92
16	214031	209.65	45.61	4.60	220.87	34.25	6.45	222.75	32.44	7.03
17	214032	182.99	65.64	2.87	99.66	24.64	4.05	106.70	18.36	5.81
18	214033	155.76	89.28	1.81	163.03	78.99	2.06	138.45	107.95	1.31
19	214040	210.74	41.89	5.23	181.78	68.13	2.67	192.82	59.20	3.40
20	214041	178.07	66.52	2.74	76.41	142.30	0.54	219.63	34.11	6.77
21	214045	180.81	72.57	2.53	150.27	101.52	1.48	187.61	65.02	3.12
22	214047	185.11	66.27	2.97	169.88	75.62	2.25	179.93	71.13	2.90
23	214048	200.89	51.84	4.02	175.80	75.56	2.33	184.77	66.19	3.03
24	214049	164.82	85.79	2.10	114.95	130.46	0.88	140.33	108.16	1.38
25	214050	184.09	67.02	2.80	195.43	55.79	3.50	178.24	75.17	2.37
26	214058	184.66	63.91	2.96	146.77	95.96	1.53	187.19	60.91	3.25
27	214062	145.73	103.35	1.52	-	-	-	-	-	-
28	214065	94.96	31.30	3.58	83.77	42.76	2.14	97.81	28.98	3.62
29	214066	165.96	85.44	2.01	182.25	67.61	2.70	161.40	90.36	1.83
30	214067	180.27	71.84	2.56	172.80	77.63	2.23	209.21	43.67	5.69
31	214075	196.30	54.37	3.75	159.39	87.12	1.83	180.43	69.59	2.83
32	214077	187.43	63.94	3.32	161.28	86.45	1.87	193.93	59.08	3.53
33	214078	125.82	123.20	1.08	161.37	89.99	1.79	132.43	114.90	1.26
34	214080	162.36	87.52	1.94	169.40	77.19	2.19	204.86	46.24	4.45
35	214084	159.49	87.59	1.85	208.03	44.41	4.68	152.62	95.66	1.63
	Mean:	169.93	66.13	2.92	154.82	63.08	2.69	171.45	68.90	2.88
	St.Dev:	31.24	18.80	0.86	38.45	22.74	0.83	31.42	22.55	0.94

Table 5.15: Results of power spectral analysis of SBPV from controls group using BT method ($mmHg^2/Hz$). No Significance within controls, $p>0.05$. †: $p<0.05$ cf. patients.

Results of Power Spectral Analysis of SBPV from Patients: BT Method										
		BASELINE			TONIC			POST		
	SUBJECT ID.	LF	HF	LF:HF RATIO	LF	HF	LF:HF RATIO	LF	HF	LF:HF RATIO
1	114016	212.86	40.34	5.35	216.04	37.92	5.70	204.97	48.34	4.53
2	114021	169.90	77.43	2.56	159.32	87.55	1.82	182.01	66.57	3.23
3	114022	165.04	82.93	2.13	186.17	65.59	2.84	163.75	86.99	2.14
4	114023	157.82	91.15	1.74	219.22	34.80	6.30	167.08	83.00	2.06
5	114024	110.10	134.95	0.89	105.91	140.24	0.76	160.80	85.58	1.91
6	114029	151.74	101.26	1.64	100.19	24.56	4.08	94.19	32.18	2.93
7	114034	179.22	71.21	2.59	191.09	53.67	3.56	171.54	77.76	2.26
8	114036	176.16	72.24	2.48	203.47	49.38	4.12	197.00	55.70	3.74
9	114037	178.05	73.28	2.54	180.35	68.56	2.63	182.76	68.33	2.95
10	114039	203.47	49.31	4.29	166.44	84.33	1.97	213.61	39.97	5.54
11	114043	96.72	151.17	0.65	175.08	72.87	2.40	137.79	113.64	1.32
12	114052	139.51	112.98	1.25	96.21	150.94	0.64	164.94	88.23	2.04
13	114053	216.78	36.85	6.46	209.39	42.50	4.93	221.29	32.61	7.00
14	114055	181.75	70.28	2.71	139.00	105.34	1.32	166.26	84.69	2.08
15	114056	205.81	48.59	4.36	105.26	21.61	4.87	-	-	-
16	114059	184.04	68.12	2.84	-	-	-	-	-	-
17	114063	117.24	130.67	0.93	54.07	194.01	0.28	102.13	146.25	0.75
18	114064	170.43	80.47	2.29	-	-	-	-	-	-
19	114071	148.27	100.44	1.58	188.31	62.19	3.03	-	-	-
20	114073	111.36	130.46	0.86	58.77	62.38	0.94	-	-	-
21	114076	186.36	66.82	3.38	162.72	88.81	1.83	168.52	82.02	2.07
22	114081	215.71	36.34	6.17	199.95	49.56	4.03	174.58	74.56	2.44
	Mean:	168.00	82.38	2.83	158.08	68.40	3.05	172.02	69.39	3.09
	St.Dev:	62.06	41.06	1.76	68.69	40.78	1.74	67.28	33.06	1.63

Table 5.16: Results of power spectral analysis of SBPV from patient group using BT method ($mmHg^2/Hz$). No Significance, $p>0.05$. Highlighted patients were from the diarrhea group and not used in the computation.

5.5 RESULTS OF WIGNER-VILLE ANALYSIS OF HRV SIGNAL FROM A CONTROL SUBJECT

Wigner-Ville decomposition was used to observe the change in the continuous power spectra as the HRV signal progressed from the baseline, ramp, tonic and post-distention states. However, it was difficult to correlate instantaneous values of the Wigner-Ville power spectra with sympathetic and parasympathetic components of the ANS and a qualitative description of the analysis is given below, for a healthy control. The graphs in figure 7.1 show the computed Wigner-Ville power spectra of a healthy control subject.

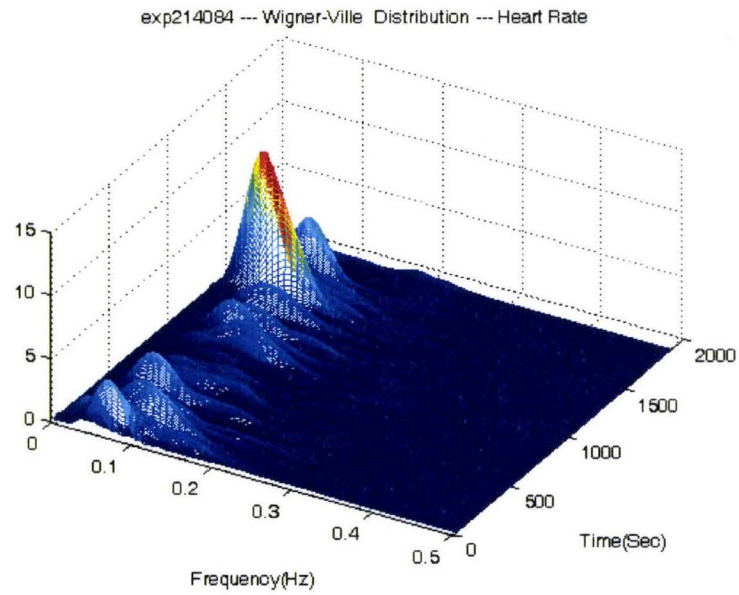

Figure 5.1(a): Wignerville time-frequency power spectra graph for a healthy control

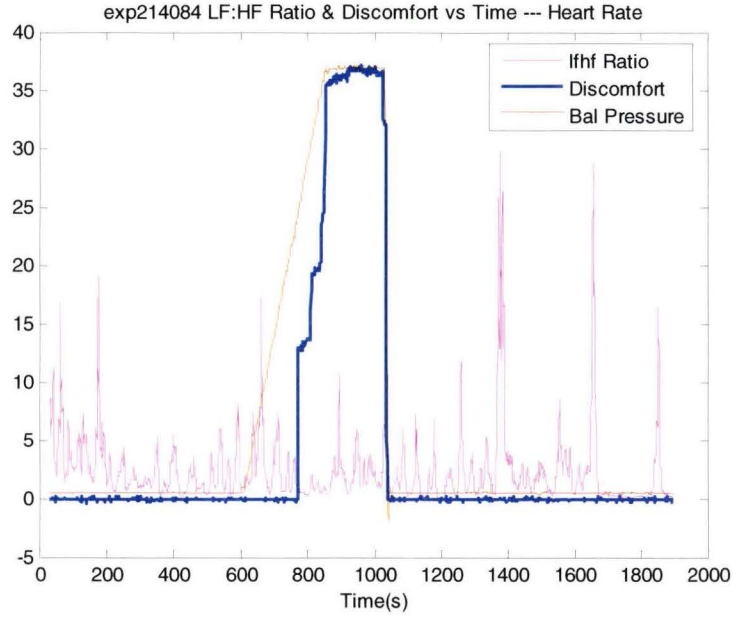

Figure 5.1(b): Superposition of LF:HF ratio, balloon pressure, and discomfort (axis scaled for convenience)

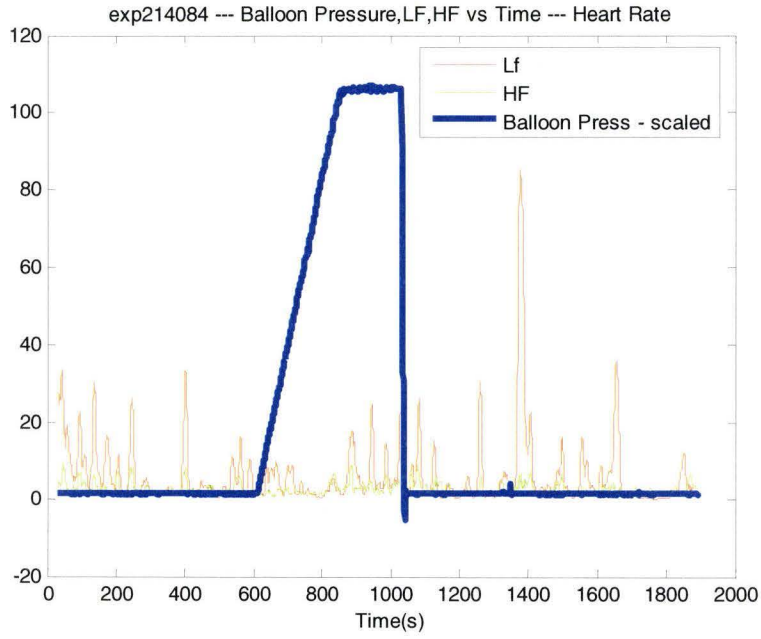

Figure 5.1(c): Superposition of LF, HF, and balloon pressure

From the above figure it can be seen that during the ramp state and tonic state, there was a decrease in the LF power and HF power, which resulted in a lower LF:HF ratio.

5.6 SUMMARY

In this chapter we outlined results obtained from our studies. These results demonstrate that ANS indices may permit one to gain insights into the functioning of GI organ system of healthy controls and patients with IBS.

Chapter 6

DISCUSSION

6.1 INTRODUCTION

In this chapter, methodological aspects arising out of hemodynamic signal processing during gastrointestinal stimulation in healthy controls and patients issues will be discussed. Secondly, the relevance of applying these methods in patients with IBS will also be examined. Finally, the results of these studies will be evaluated for applications in IBS research.

6.2 ISSUES OF DIGITAL SIGNAL PROCESSING OF HEMODYNAMIC SIGNALS

The sampling rate for all variables reported in this thesis was set at 500 samples/second. Since both ECG and BP signals have spectral components well below 100 Hz, the

sampling rate was deemed to be adequate. The A/D converter had 16 bit resolution and would be considered standard sampling resolution in most laboratories. The filtering was performed using finite impulse response algorithms (FIR) developed by MATLAB and have linear phase property for the frequency range of interest. Algorithms employed for power spectral analysis have been based on well known sources (11).Both Blackman-Tukey and AR methods have different theoretical basis. While the former assumes an infinitely long signal, the autoregressive method fits a model to the available signal. Therefore, fewer data points are needed. While other groups may use about 4 minutes of heart rate signal to compute the power spectra, 128 seconds of data has been found to be adequate. In general, a minimum of three minutes of hemodynamic signal data are available during shortest (tonic) phase of the study and would suffice for the present work. BT and AR methods of computing power spectra did not always generate identical results. Wigner-Ville algorithm can generate qualitative data for identifying how the patient responds using three-dimensional displays. Quantitative indices are not easily interpreted.

6.3 NOVELTY OF THE RESEARCH

The work reported in this thesis is novel, because there is no reported use of BRS and power spectral methods during an intervention such as colorectal distention. Comparison of BRS methods has been done by a number of investigators [16] but no publication has examined the use of balloon distention as a source of perturbation of the GI system and simultaneously quantifying the autonomic nervous system. It is also an attempt to simulate symptoms of bloating and fullness experienced by patients with IBS. Therefore, methods and results reported in this thesis are directly applicable in a clinical

situation and may assist the physician in better understanding the pathophysiology of IBS.

6.4 METHODOLOGICAL ISSUES OF COMPUTINGTHE BRS

There is considerable controversy in the literature regarding how the BRS is computed and interpreted. Only salient points arising out of the results presented herein,

6.4.1 Invasive vs Non-invasive methods

During the early years of measuring the BRS, a bolus of a vasodilation drug such as phenylephrine (vasoconstrictor) was administered and the hemodynamic response (R-R intervals and BP values) were measured by an invasive pressure transducer [28]. . Since the development of Finometer, the non-invasive method of computing the BRS has gained acceptance in physiological and clinical literature. Many international laboratories use the instrument in their routine physiological research. A recent article by Dr.Taylor's group [16] critically evaluated these methods and concluded that clinician should not overly rely on BRS values obtained from such algorithms, especially to provide critical clinical guidance. Secondly, it is likely that information gathered about BRS by non-invasive blood pressure may not reflect true blood pressure. Finally, it is also claimed that pharmacological agents such as Pheneylephrine or Nitroprsusside (vasodilator) may modify the very responses one wishes to study. Therefore, one can argue that the interpretation of measurement of BRS in a clinical setting is not always straightforward.

6.4.2 Algorithms for computing the BRS

Lippman et al. [16] identifiy five algorithms and compares the BRS values obtained using each method. Four of these methods are based on frequency analysis (i.e. transfer function analysis, cross-spectral analysis etc.) and the fifth method is based on time-domain method of identifying sequential increase (decrease) of R-R intervals and blood pressure. While arguments can be made for each method, the frequency domain methods are indirect at best and the BRS (ms/ mm Hg) is determined by dimensional analysis [16]. Therefore, results obtained in this thesis are important because they show a trend which is not affected by methodological differences. And these trends may be useful while studying IBS patients before or following a clinical intervention (eg: drugs or stress reduction).

6.5 PHYSIOLOGICAL AND CLINICAL IMPLICATIONS

Research reported in this thesis has applications in physiology and clinical medicine. Hemodynamic signals are affected by dysfunction or invasive interventions such colorectal balloon distention. The efferent signals generated in response to such afferent input are sympathetically dominant. It is envisaged that various parameters studied in this thesis may help clinical physiologist in understanding the IBS and effect of therapies where ANS is affected.

Results reported in this thesis demonstrate that BRS can act as dynamic parameters to characterize patients with IBS. Based on the observations outlined earlier, it is imperative that patients have lower BRS and therefore respond poorly to homeostatic demands made by major organs within the body. It is well documented that the BRS is a clinically relevant predictor of cardiovascular medicine [14]. In the area of IBS, the BRS may serve

as a marker of the ANS health. It is not known if BRS is correlated with the severity of IBS, a question suitable for a clinical scholar interested in this issue. Also, BRS may serve to quantify the effectiveness of medications which ameliorate symptoms of IBS. While the power spectral analysis did not yield any concrete results of significance, it is likely that adaptation processes taking place in the GI system during slow rectal distention may be reducing the sensitivity of power spectral analysis of the HRV and BPV signals. This is an area where a dynamic parameter may yield more meaningful results.

Chapter 7

Limitations and Conclusion

7.1 LIMITATIONS OF THE STUDY

In this section some limitations of the study will be outlined.

a. In the present work there were no age matched volunteers for comparing results with patients, limitations that can be overcome in the future. Further, healthy women in their 40s and 50s are not easy to recruit for the study.

b. IBS patients fall into one of the constipated, diarrhea or alternating groups. We need more patients in each of the above classes to obtain clinically useful information.

c. Reproducibility of results on the same patient may be one of the issues that needs to be studied.

d. The paradigm used is effective in emulating the bowel (filling and motility). However, the ANS and GI system time constants do not match, as such, a quicker inflation of the balloon may be needed to improve results.

7.2 CONCLUSIONS

In this thesis, a computer controlled barostat was used to inflate a balloon in the human rectum as a model for irritable bowel syndrome. A number of healthy controls (n =35) and IBS patients (n=22) were studied. The protocol designed was to create discomfort in the subject which was similar to the bloating sensation felt during an episode of IBS. These studies demonstrate that there is a downward shift in the baroreceptor sensitivity in patients with constipated IBS. Results of power spectral analysis on the HRV using BT and AR methods gave slightly differing results. However, baroreceptor sensitivity emerged as a useful dynamic parameter to differentiate between rest, ramp, tonic and post-distention states.

A hypothesis can be stated that there may be mechano-receptors in the bowel. Therefore the BRS results may show valid results with respect to a sympathetic overdrive and vagal impairment.

REFERENCES

[1] Amaral L. A., Goldberger A. L., Ivanov P. CH., Stanley H. E., "Modeling heart rate variability by stochastic feedback," Computer Physics Communications vol.121-122: 126-128(1999).

[2] Badra L. J., Cooke W. H., Hoag J. B., Crossman A. A., Kuusela T. A., Tahvanainen K. U. O., Ickberg D. L., "Respiratory modulation of human autonomic rhythms," Am J Physiol Heart Circ Physiol **280**: H2674-H2688 (2001).

[3] Barbieri E., Parati G., Saul J. P., "Closed-versus Open-Loop Assessment of Heart Rate Baroreflex," IEEE Engineering in Medicine and Biology: 33-42 (March/April 2001).

[4] Berger R. D., Saul J. P., Cohen R. J., "Tansfer function analysis of autonomic regulations I. Canine atrial rate response," The American Physiological Society : H142-H152 (1989).

[5] Blasi A., Jo J., Valladares E., Morgan B. J., Skatrud J. B., Khoo M. C. K., Cardiovascular variability after arousal from sleep: time-varying spectral analysis, J Appl Physiol 95: 1394-1404 (2003).

[6]. Bouin M, Plourde V, Boivin M, Riberday M, Lpaien F, Langniere M, Verrier P and Poitras, P.l Rectal distention testing in patients with irritable bowel syndrome: sensitivity, specificity, and predictive values of pain sensory thresholds. Gastroenterology, 122:1771-1777, 2002.

[7] Freitas J., Pereira S., Lago P., Costa O., Carvalho J., Falcao de Freitas A., "Impaired arterial baroreceptor sensitivity before tilt-induced syncope," Europace **1**: 258-265 (1999).

[8] Huang N. E., Shen Z., Long S. R., Wu M. C., Shih H. H., Zheng Q., Yen N.C, Tung C.C., and Liu H. H. *The empirical mode decomposition and the Hilbert spectrum for nonlinear and non-stationary time series analysis.* Great Britain: The Royal Society, 1998.

[9] Kamath M. V., Fallen E. L., "Power Spectral Analysis of Heart Rate Variability: A Noninvasive Signature of Cardiac Autonomic Function," Critical Reviews in Biomedical Engineering **21**(3): 245-311 (1993).

[10] Kardos A. Watterich G. De Menezes R. Csanady M. Casadei B. Rudas L. *Determinants of spontaneous baroreflex sensitivity in a healthy working population.* Hypertension, Vol. 37(3)(pp 911-916), 2001.

[11] Kay S. M., *Modern spectral estimation: theory and application*, Prentice Hall. 1988.

[12] Korhonen I., "Multivariate closed-loop model for analuses of cardiovascular dynamics," Meth Inform Med **36**: 264-267 (1997).

[13] Kornet L. Hoeks APG. Janssen BJA. Houben AJ. De Leeuw PW. Reneman RS. *Neural activity of the cardiac baroreflex decreases with age in normotensive and hypertensive subjects.* Journal of Hypertension, Vol. 23(4)(pp 815-823), 2005.

[14] La Rovere MT, Bigger JT, Marcus FI, Mortara A, Schwartz PJ. Baroreflex sensitivity and heart rate variability in prediction of total cardiac mortality after myocardial infarction:ATARMI. Lancet: 351:478-484, 1998.

[15] Lantelme P. Khettab F. Custaud M-A. Rial M-O. Joanny C. Gharib C. Milon H. *Spontaneous baroreflex sensitivity: Toward an ideal index of cardiovascular risk in hypertension?.* Journal of Hypertension, Vol. 20(5)(pp 935-944), 2002.

[16] Lippman R, Salisbury J and Taylor JA. Spontaneous indices are inconsistent with arterial baroreflex gain. Journal of Hypertension, 2003:42:481-487.

[17] Lorena S. L. S., Figueiredo M. J. O., Almeida J. R. S., Mesquita M. A., "Autonomic Function in Patients with Functional Dyspepsia Assessed by 24-hour Heart Rate Variability," Digestive Diseases and Sciences **47** (1): 27-31 (January 2003).

[178] Mertz HR. Irritable Bowel Syndrome.The NewEngland Journal of Medicine.2003:349,2136-2146.

[19] Monahan KD. Dinenno FA. Seals DR. Clevenger CM. Desouza CA. Tanaka H. *Age-associated changes in cardiovagal baroreflex sensitivity are related to central arterial compliance.* American Journal of Physiology - Heart & Circulatory Physiology, Vol. 281(1 50-1)(pp H284-H289), 2001.

[20] Mullen T. J., Appel M. L., Mukkamala R., Mathias J. M., Cohen R. J., "System identification of closed-loop cardiovascular control: effects of posture and autonomic blockade," Am J Physiol Heart Circ Physiol 272: H448-H461, (1997).

[21] Parati G., Di Rienzo M., Omboni S., Mancia G., Computer analysis of blood pressure and heart rate variability in subjects with normal and abnormal autonomic cardiovascular control, Autonomic Failure: A Textbook of Clinical Disorders of the Autonomic Nervous System. Editors: J. Mathias, R. Bannister. (Oxford) pp.211-223, 1999

[22] Peckerman A. Hurwitz BE. Nagel JH. Leitten C. Agatston AS. Schneiderman N. *Effects of gender and age on the cardiac baroreceptor reflex in hypertension.* New York: Clinical & Experimental Hypertension, Vol. 23(8)(pp 645-656), 2001.

[23] Pola S., Macerata A., Emdin M., Marchesi C., "Estimation of the Power Spectral

Density in Nonstationary Cardiovascular Time Series: Assessing the Role of the Time-Frequency Representations (TFR)," IEEE Transactions on Biomedical Engineering **43**(1): 46-59 (Jan. 1996).

[24] Rilling G., Flandrin P. and Gonçalvès P. *On Empirical Mode Decomposition and its Algorithms.* (http://www.inrialpes.fr/is2/people/pgoncalv/pub/emd-eurasip03.pdf).

[25] Ruha A, Sallinen S and Nissla S. A real-time microprocessor QRS detector system with a 1-ms timing accuracy for the measurement of ambulatory HRV. IEEE Trans.Biomed. Eng. Mar; 44(3):159-67. 1997.

[26] Saul J. P., Berger R. D., Albrecht P., Stein S. P., Chen M. H., Choen R. J., "Transfer function analysis of the circulation: unique insights into cardiovascular regulations, American Journal Physiology: H1231-H1245 (1991).

[27] Saul J. P., Berger R. D., Chen M. H., Cohen R. J., "Transfer function analysis of autonomic regulation II. Respiratory sinus arrhythmia, American Journal Physiology: H153-H161 (1989).

[28] Smyth HS, Sleight P, Pickering GW. Reflex regulation of arterial pressure during sleep in man. A quantitative method of assessing baroreflex sensitivity, Circulation Research, 1969: 24:109-121.

[29] Waring W. S., Chui M., Japp A., Nicol E.F., Ford M. J., Autonomic cardiovascular responses are impaired in women with irritable bowel syndrome. Journal of Clinical Gastroenterology. 38(8): 658-663, September 2004.

[30] Watkins L. L., Grossman P., Sherwood A., "Noninvasive Assessment of Barorflex Control in Borderline Hypertension Comparison With the Phenylephrine Method," Hypertension 28: 238-243 (1996).

[31] Wesseling, Karel H. Should baroreflex sensitivity be corrected for heart rate? Journal of Hypertension: Volume 21(11): 2015-2018 , November 2003.

APPENDIX A:

Empirical Mode Decomposition Method

A.1 INTRODUCTION

Empirical Mode Decomposition, or EMD for short, is a new, and very unique technique developed for signal processing by Huang [8]. The most important factor in this technique is that it works on non-linear, non-stationary data, and is able to decompose any complicated data set into a finite, often small number of 'intrinsic mode functions'. These intrinsic mode functions (IMFs) admit well-behaved Hilbert transforms, and yield instantaneous frequencies as functions of time that give sharp identifications of imbedded structures. This means that the IMFs allow for the interpretation of physical meaning to components within a complex wave that were previously unavailable. Finally, because EMD is adaptive, it is able to provide all of this functionality in an extremely efficient manner.

A.2 EMD- THE PROCESS

In order for the EMD method to be applied, the following assumptions must hold true: (1) the signal has at least two extrema- one maximum and one minimum; (2) the characteristic time scale is defined by the time lapse between the extrema; and (3) if the data were totally devoid of extrema but contained only inflection points, then it can be differentiated once or more times to reveal the extrema. Final results can be obtained by integration(s) of the components.

The essence of the method is to identify the intrinsic oscillatory modes by their characteristic time scales in the data empirically, and then decompose the data accordingly. The time scale can be defined as either time lapse between the successive alternations of local maxima and minima; or by the time lapse between the successive

zero crossings. Most researchers have decided to adopt the time lapse between successive extrema as the definition of the time scale for the intrinsic oscillatory mode, because it not only gives a much finer resolution of the oscillatory modes, but also can be applied to data with non-zero mean, either all positive or all negative values, without zero crossings. A systematic way to extract them, designated as the sifting process, is described by Huang [8].

A.3 APPLICATIONS:

It is instructive to examine samples from literature [26] to see how the EMD process is performed. Figure 7.1 from [26] provides an example of how well EMD can decompose a non-linear signal into a series of IMFs that have clear physical significance. This figure shows an excellent example of the use of EMD, because the human eye can clearly see the 3 components that made up this signal. The first IMF corresponds to the finest local mode (or the highest frequency). The next two successively correspond to less fine local modes. Also note that the remaining residual is constant at 0. If our dataset contained a trend, then our residual would correspond to that trend.

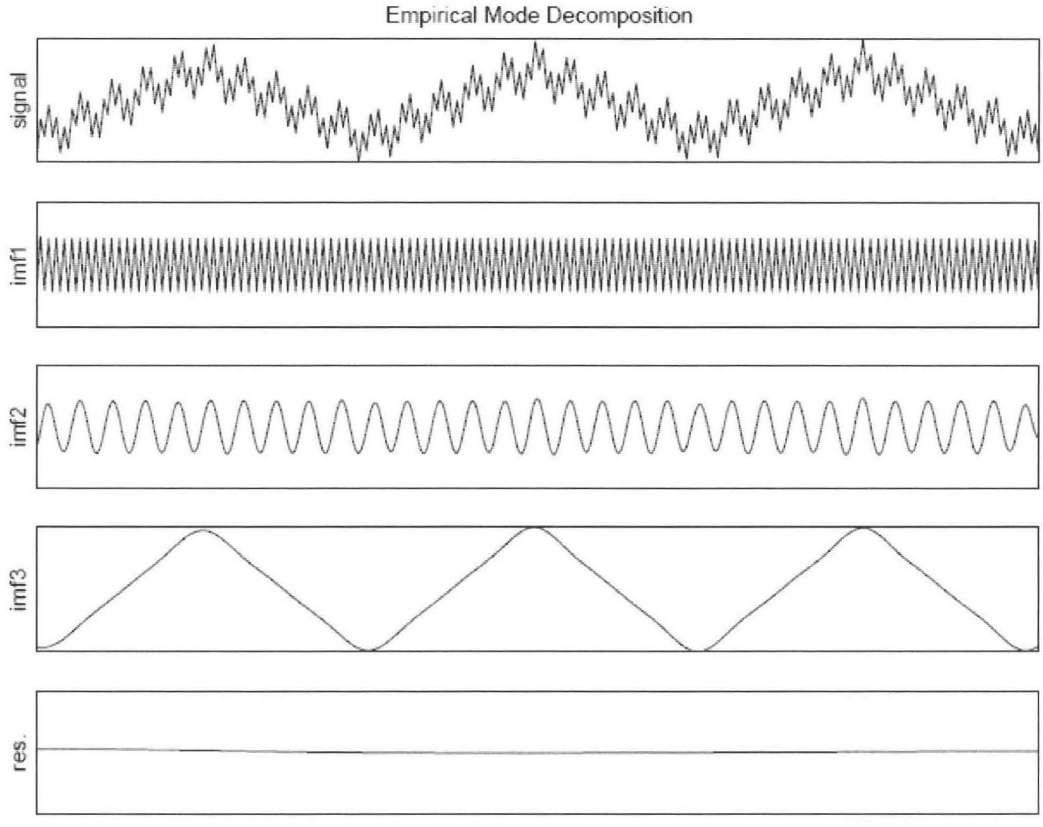

Figure A.1: Application of EMD to a non-linear signal

A.4 LIMITATIONS OF EMD:

One of the major issues with EMD is that it is susceptible to errors due to sampling, especially when dealing with only a few points per period. Take, for example, a pure tone. One would expect that that EMD would provide the unity operation, that is, to return only one IMF that was the original tone, with a 0 residue. However, when this tone is sampled, it may create jittered extrema, resulting in an incorrect extrapolation.

A.5 DEVELOPMENT AND TESTING OF AN EMD ALGORITHM

The EMD algorithm was developed for this work and tested on a composite signal containing two sine waves on two sinusoids combined with a 1:1 ratio with frequencies of 0.25 Hz and 0.50 Hz. Gaussian noise was added to this signal. The figures below show the results of the algorithm run on this signal. The first graph shows the raw signal and its PSD. The subsequent 15 graphs show the 15 raw IMF's and their PSDs. The PSD's of the IMF's were compared to the original inputted signals PSD. Algorithm developed herein can be applied to real world hemodynamic data.

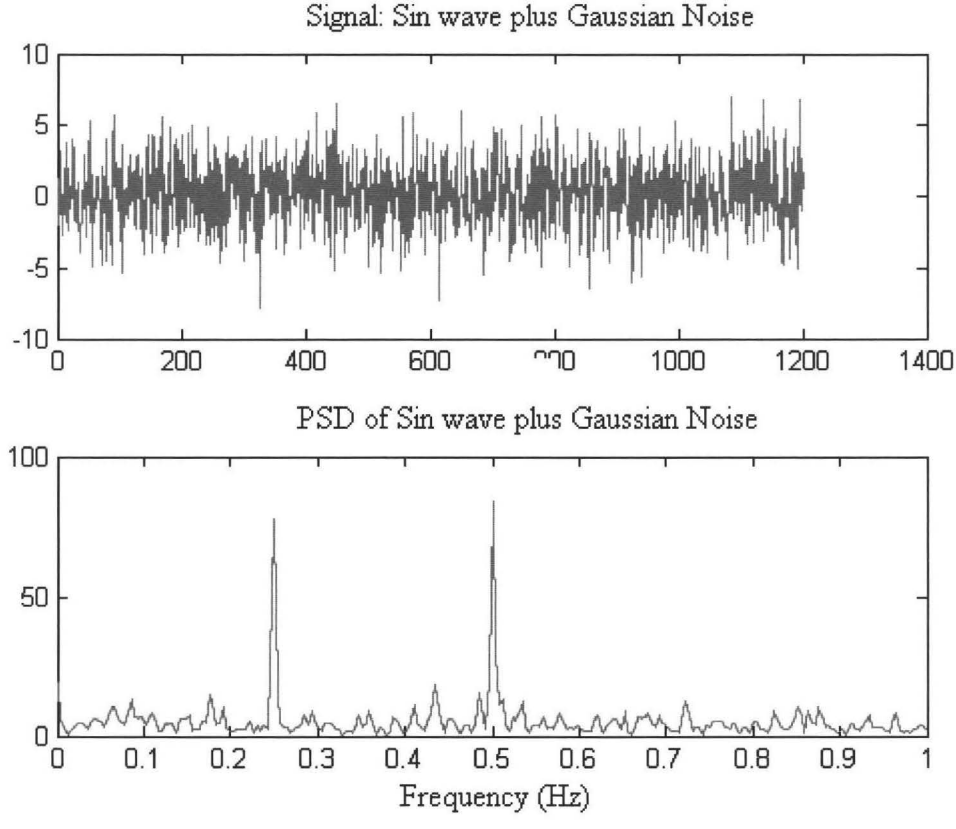

Figure A.2: Original combined signal and it's PSD

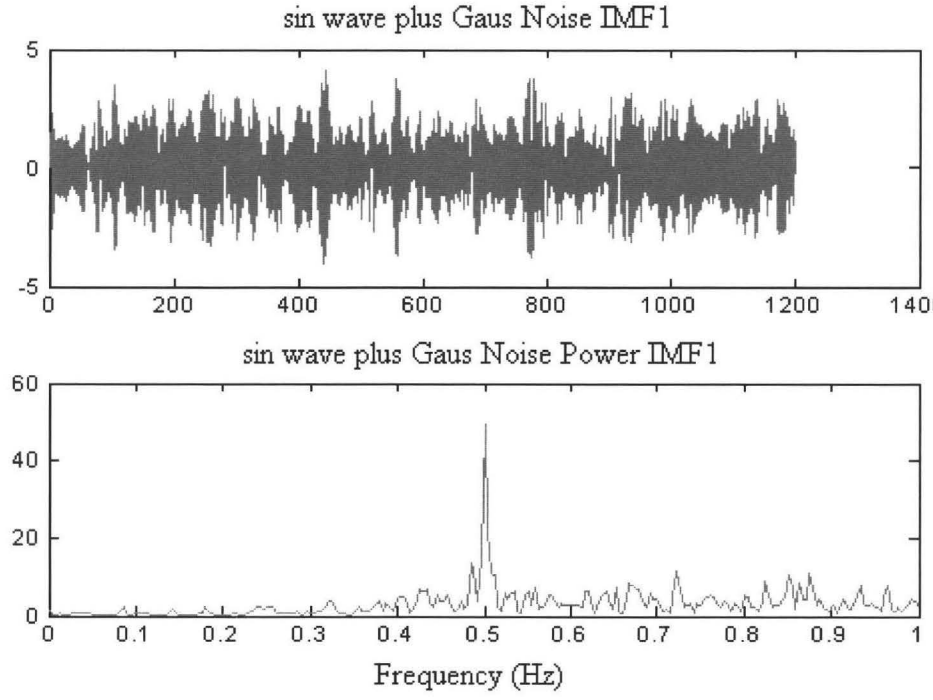

Figure A.3 (a): First IMF with its PSD

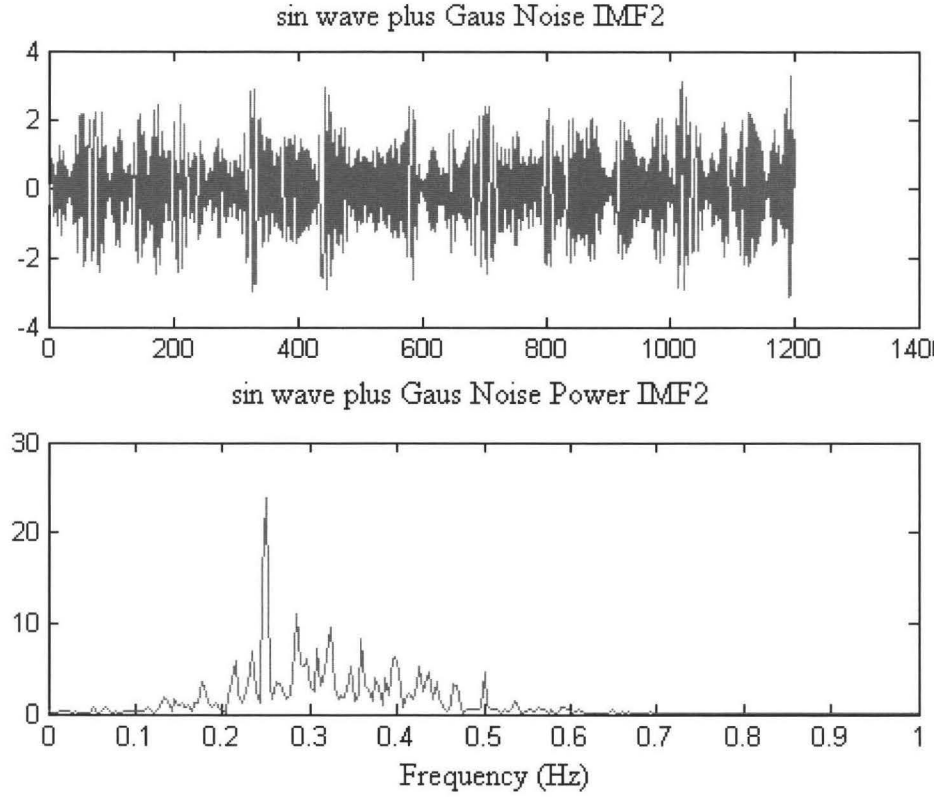

Figure A.3 (b): Second IMF with its PSD

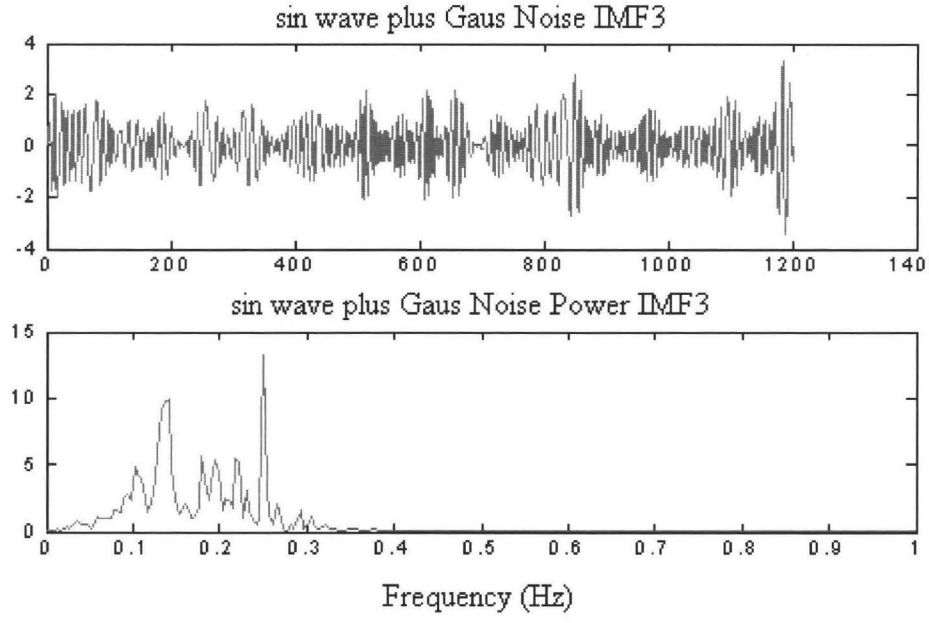

Figure A.3 (c): Third IMF with its PSD

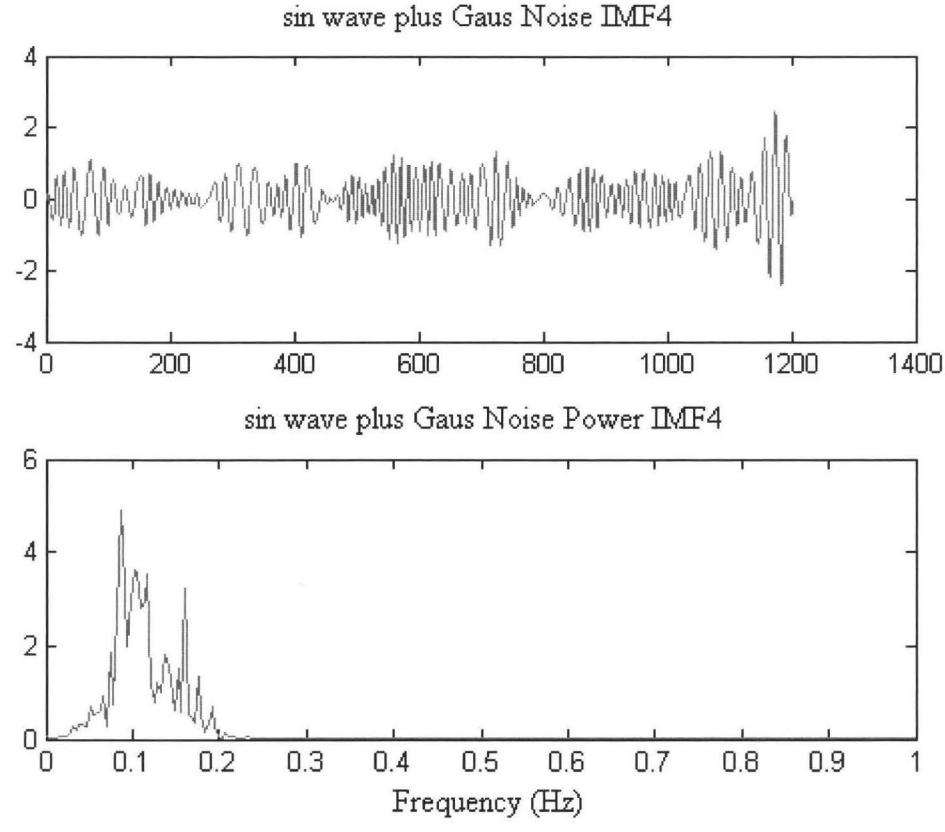

Figure A.3 (d): Fourth IMF with its PSD

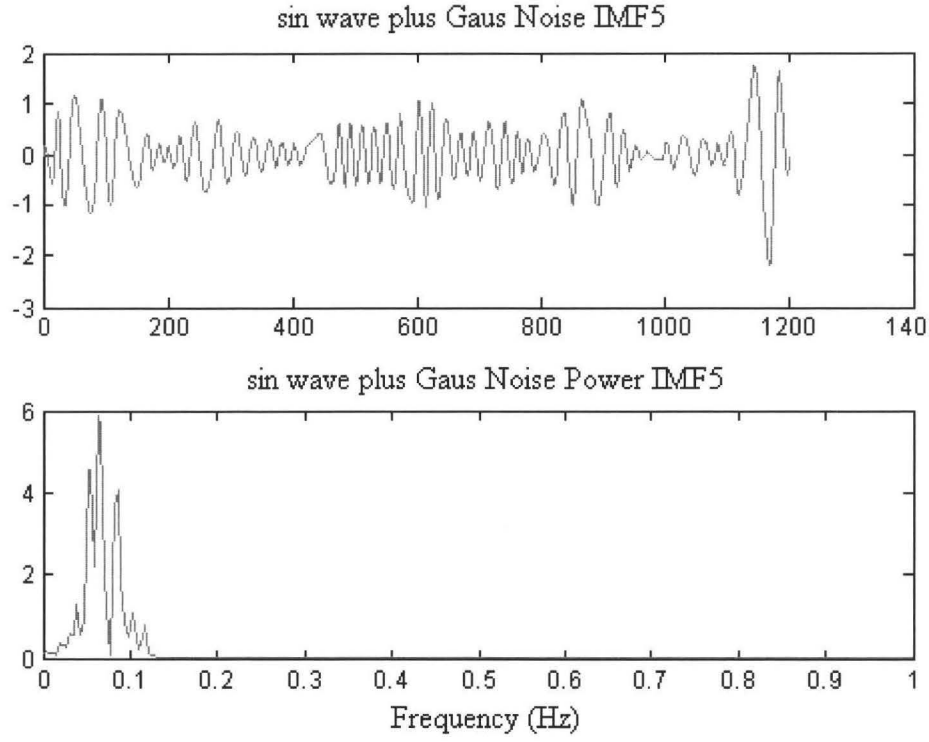

Figure A.3 (e): Fifth IMF with its PSD

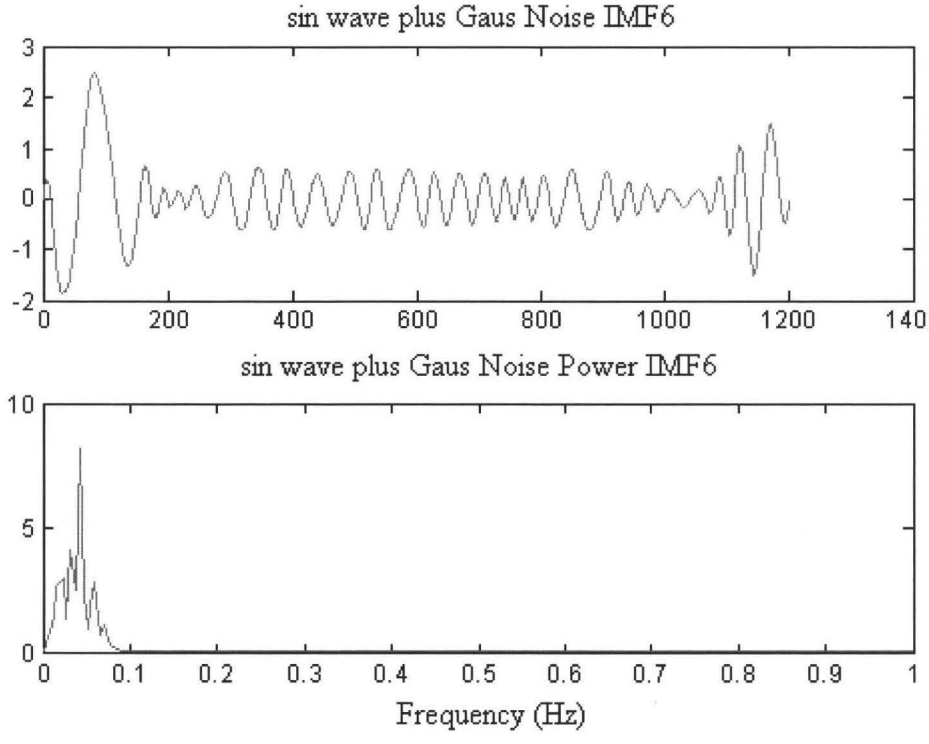

Figure A.3 (f): Sixth IMF with its PSD

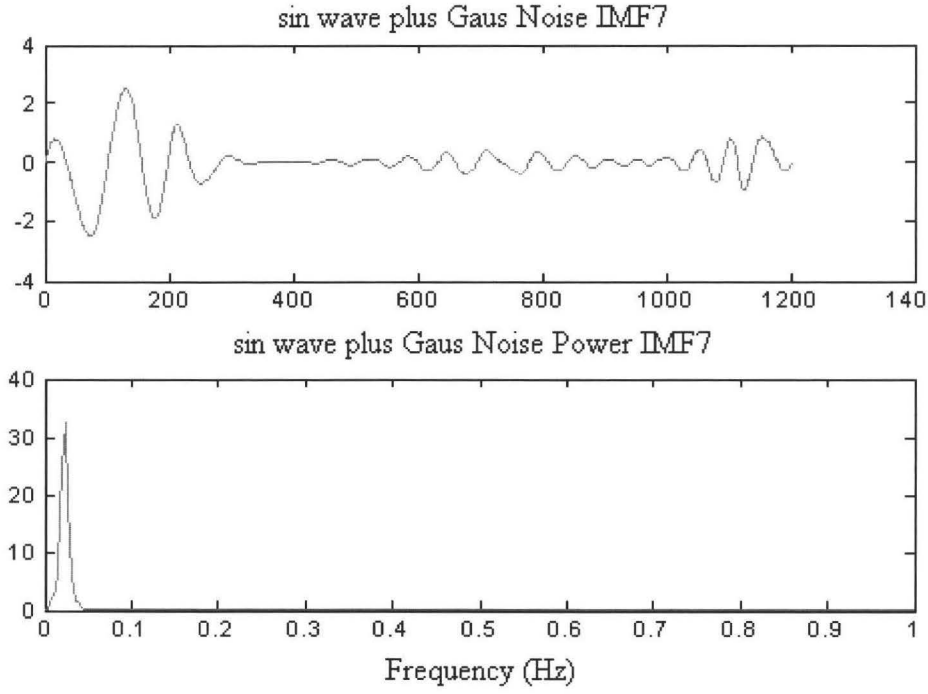

Figure A.3 (g): Seventh IMF with its PSD

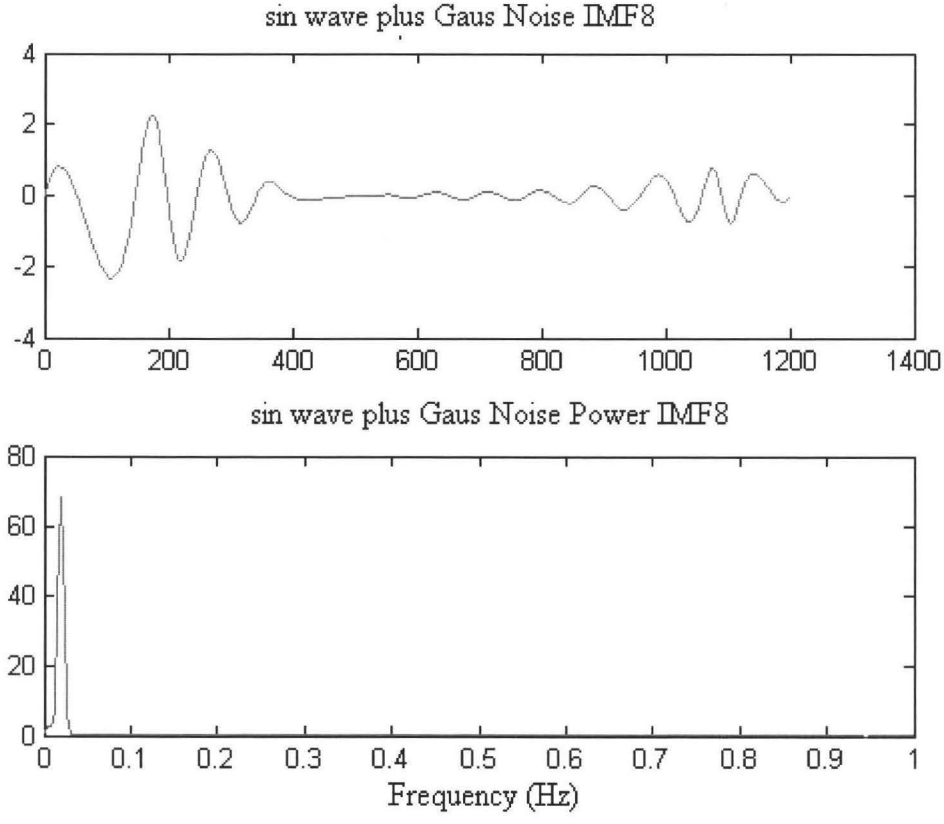

Figure A.3 (h): Eighth IMF with its PSD

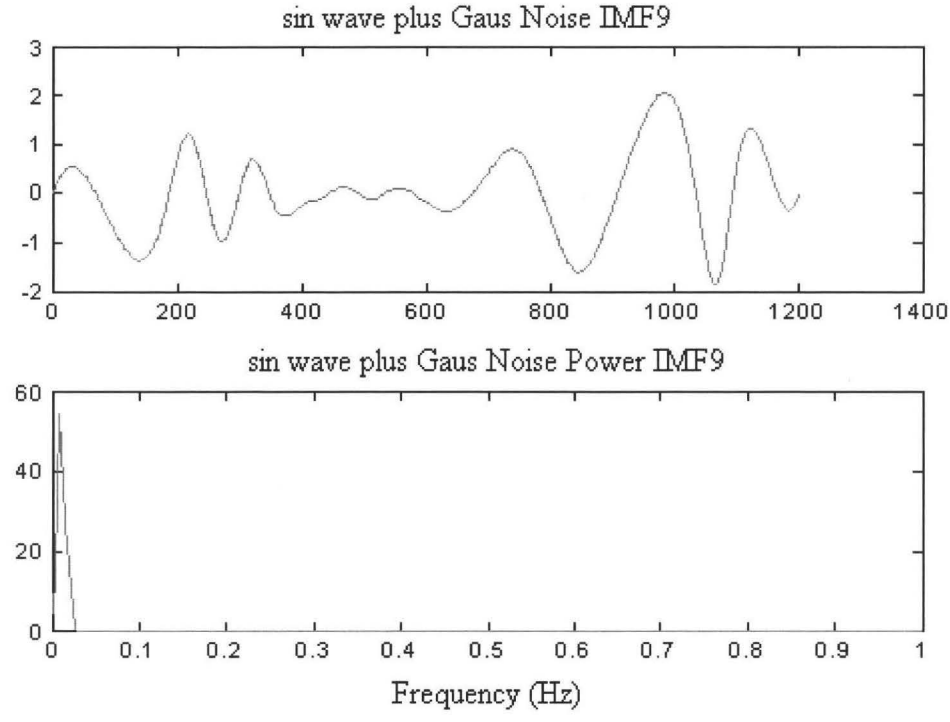

Figure A.3 (i): Ninth IMF with its PSD

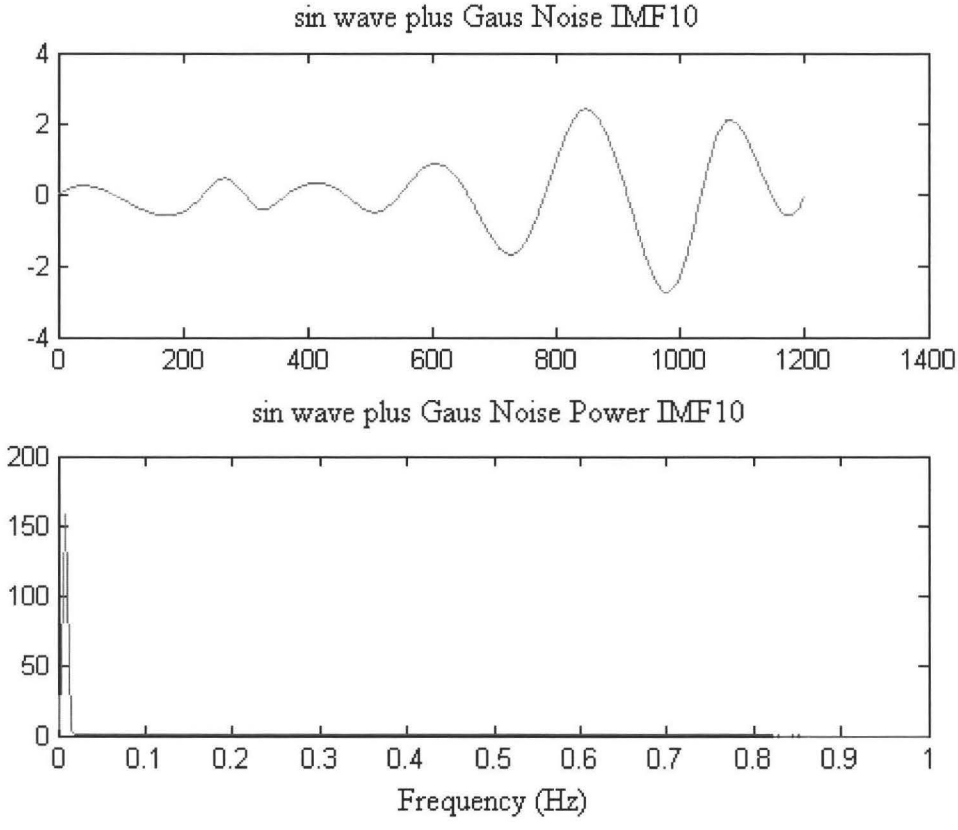

Figure A.3 (j): Tenth IMF with its PSD

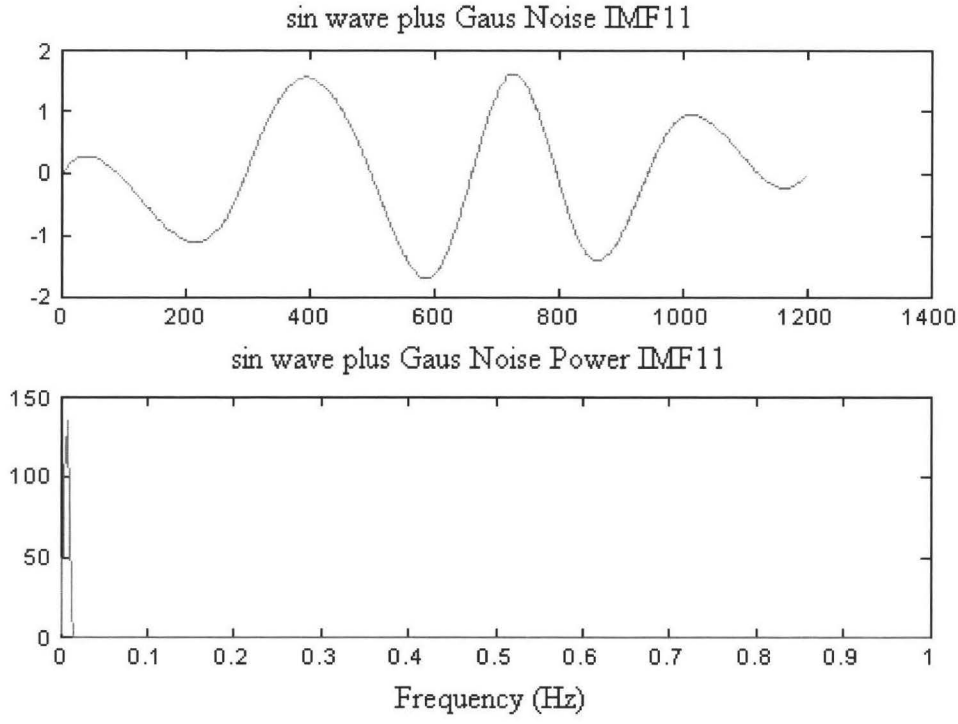

Figure A.3 (k): Eleventh IMF with its PSD

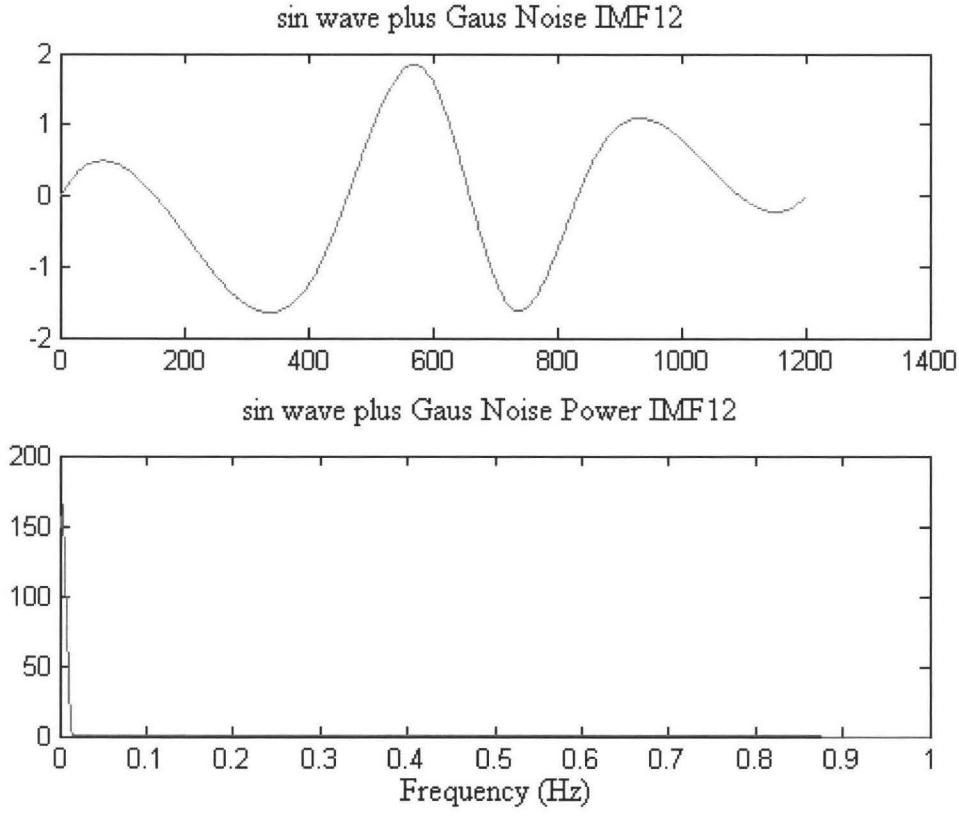

Figure A.3 (l): Twelfth IMF with its PSD

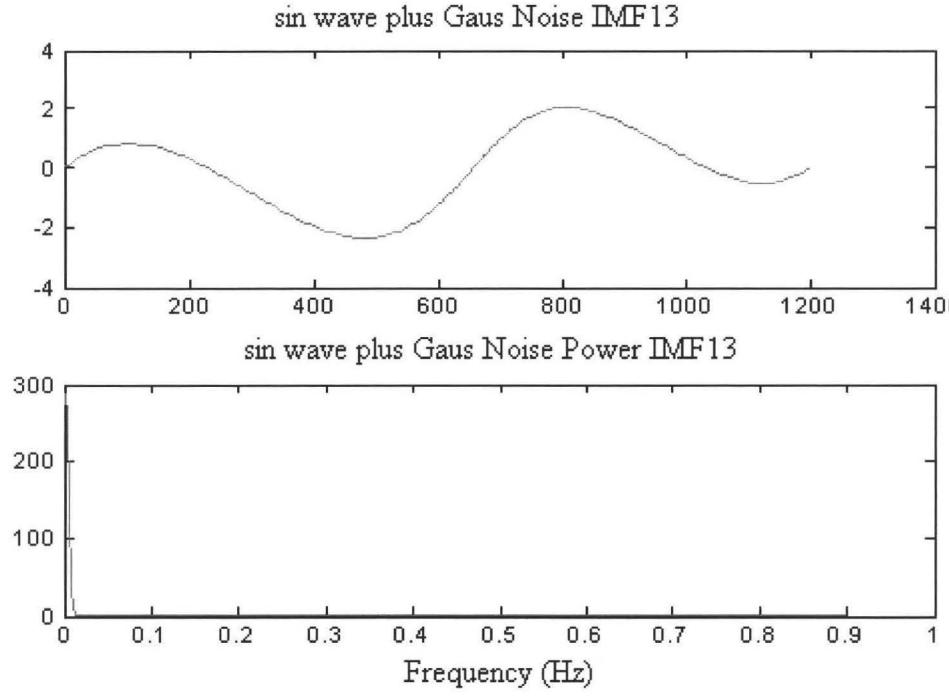

Figure A.3 (m): Thirteenth IMF with its PSD

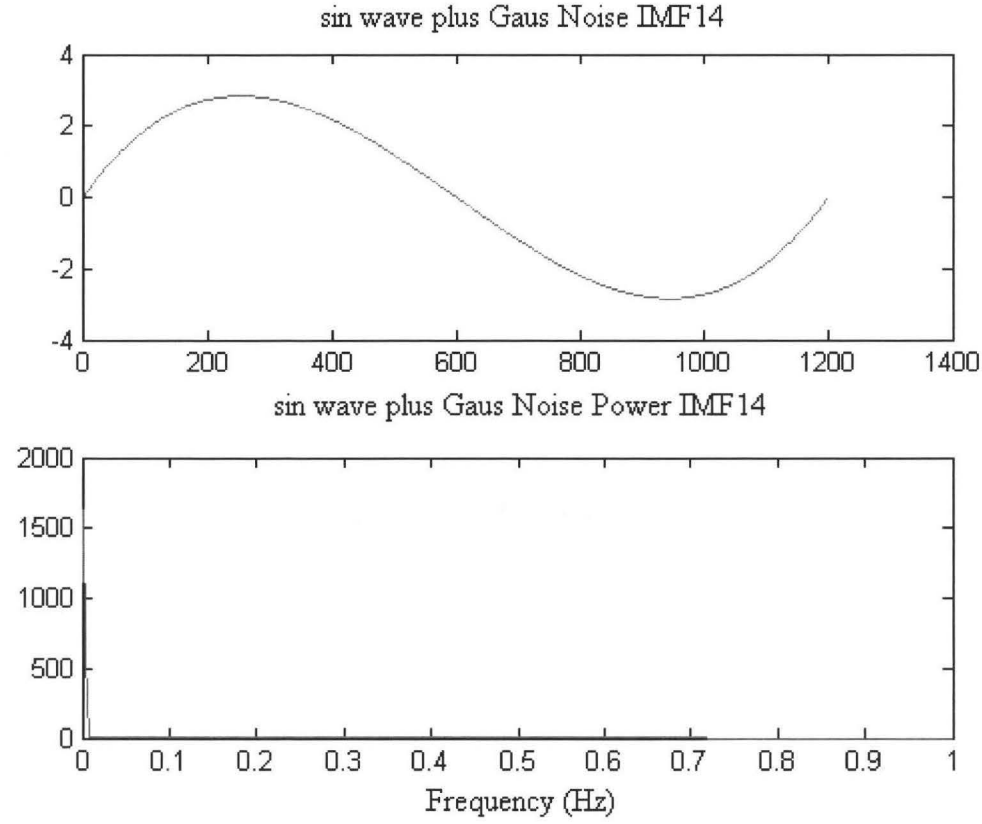

Figure A.3 (n): Fourteenth IMF with its PSD

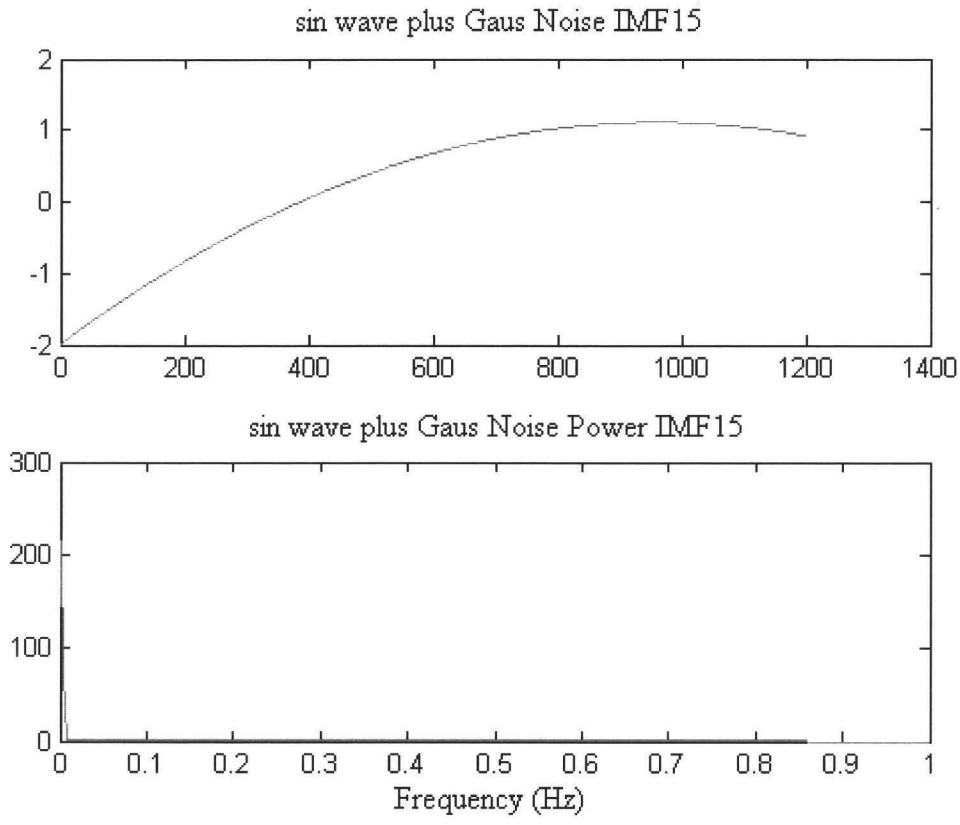

Figure A.3 (o): Fifteenth IMF with its PSD